University of Nevada, Reno

Modeling Arsenic Behavior During Artificial Aquifer Recharge

A thesis submitted in partial fulfillment of the requirements for the degree of Master of Science in Hydrogeology

By

Benjamin M. Bardet

Dr. Greg Pohll/Thesis Advisor

May 2022

THE GRADUATE SCHOOL

We recommend that the thesis
prepared under our supervision by

BENJAMIN BARDET

entitled

Modeling Arsenic Behavior During Artificial Aquifer Recharge

be accepted in partial fulfillment of the
requirements for the degree of

Master of Science

Greg Pohll, Ph.D.
Advisor

Lazaro Perez, Ph.D.
Committee Member

Rishi Parashar, Ph.D.
Graduate School Representative

David W. Zeh, Ph.D., Dean
Graduate School

May, 2022

Abstract

Increased variability in precipitation coupled with increases in population across the large portions of the western United States has resulted in greater demand being placed on this region's water resources. As a result, water conservation and storage methods are being explored to mitigate the impact that potential drought may have on these expanding population centers. Aquifer storage and recovery projects (ASR) in which excess surface water is captured and injected in local aquifers for storage, are becoming more widespread and important. As part of these programs, the use of highly treated wastewater or reclaimed water as a potential source for groundwater injection is becoming more feasible. This wastewater stream is typically underutilized if utilized at all. A hurdle in “traditional” ASR projects and particularly in reclaimed water ASR projects is understanding how these injected water’s chemistries will interact with the native groundwater and geology of the aquifer into which they are being introduced.

This study looks to identify how a numerical geochemical model framework can be used to identify potential compatibility issues between injected and native groundwaters in which degradation to overall water quality may occur. This framework is tested by looking at a case study in Reno, Nevada in which a small-scale aquifer injection test was conducted utilizing highly treated reclaimed water. In this case study, unanticipated changes in arsenic levels were observed in the aquifer during the injection test. A geochemical model was created utilizing the USGS PHREEQC modeling software to replicate batch experiments performed utilizing mineralogy collected from the Reno-Stead site. This model was used to confirm the mechanism of arsenic release at

the site as well as demonstrate its ability to understand potential mitigation measures or investigate other potential contaminants.

The results were matched with the lab and field observations and iron-oxide sorption was identified as the source and driver of arsenic mobility at the site. The developed geochemical model was able to match the observed arsenic variability at the Reno-Stead site in response to changes to injection pH values. Injection pH values in the range of 6.7-7.2 were shown to decrease arsenic concentrations below background levels. At pH values in the range of 7.1-7.4 which correspond to the actual pH values of the injection water at the site, arsenic concentrations remained relatively stable or increased slightly in response to desorption from iron-oxide surfaces caused by shifts in pH. Models run without the inclusion of iron-oxide surfaces showed no arsenic concentration changes in response to changes in injected pH and did not match the field observations from the site. This validates the hypothesis that iron-oxide sorption and desorption was the primary driver of arsenic variability observed at the Reno-Stead site.

The ability of this relatively simple geochemical framework to accurately identify and replicate observed chemistry changes at this test site proves its viability as a potential method to identify and test future sites for any compatibility issues between injected and native groundwater before significant investments of time and resources occur. While further work is needed to create a more rounded and widely applicable model, this modeling pathway allows for better understanding of the geochemical mechanisms present at recharge sites and helps direct future investigations.

Dedicated to my parents, Glenn and Cathy Bardet. Without your love and support I would not be where I am today. Thank you for everything

Contents

List of Tables

List of Figures

Introduction

a. Site Description

i. Reno-Stead Site

The Reno-Stead Water Reclamation Facility (RSWRF) is located approximately 7 miles north of Reno, NV USA. At this site, a regional team of seven public agencies jointly conducted a feasibility study to determine whether the State of Nevada's newly adopted "A+" reclaimed water category is a potentially viable water resource management tool that can be implemented in the Truckee Meadows region. In Northern Nevada and the Truckee Meadows region in particular, water resources are carefully managed to ensure water availability for all shareholders in the region. Part of this management consists of artificial aquifer recharge through the use of injection wells. This artificial recharge allows for the storage of water in the aquifer for use at a later date, most often during the drier summer months. Storage of water in the aquifer itself allows for protection from evaporation and a surface contamination that may occur in traditional reservoir storage. Historically, injected water consists of only potable water coming directly from the distribution system. The newly defined "A+" reclaimed water category allows for the investigation of the viability of this new resource as a potential new source of injection water for the region.

At the Reno-Stead site, groundwater characterization and geology samples were collected from an adjacent property owned by Truckee Meadows Water Authority (TMWA). The study site is located within the East Lemmon Valley hydrographic basin (092B) at an elevation of approximately 4,990 feet amsl (above mean sea level). On the

TMWA owned property a total of 4 wells were drilled to conduct a pilot IPR study and collect additional geologic samples. 3 of the 4 wells (LVIPR1, LVIPR2, and LVIPR3) were drilled in November 2017 for use during the pilot IPR study conducted in 2019. LVIPR1 was used as an injection well during testing, LVIPR2 was used as an intermediate monitoring point and LVIPR3 was used as an extraction well. The wells are located in line with each 40ft from the next. LVIPR4 was constructed at a later date to help understand geochemical changes that were observed at the site.

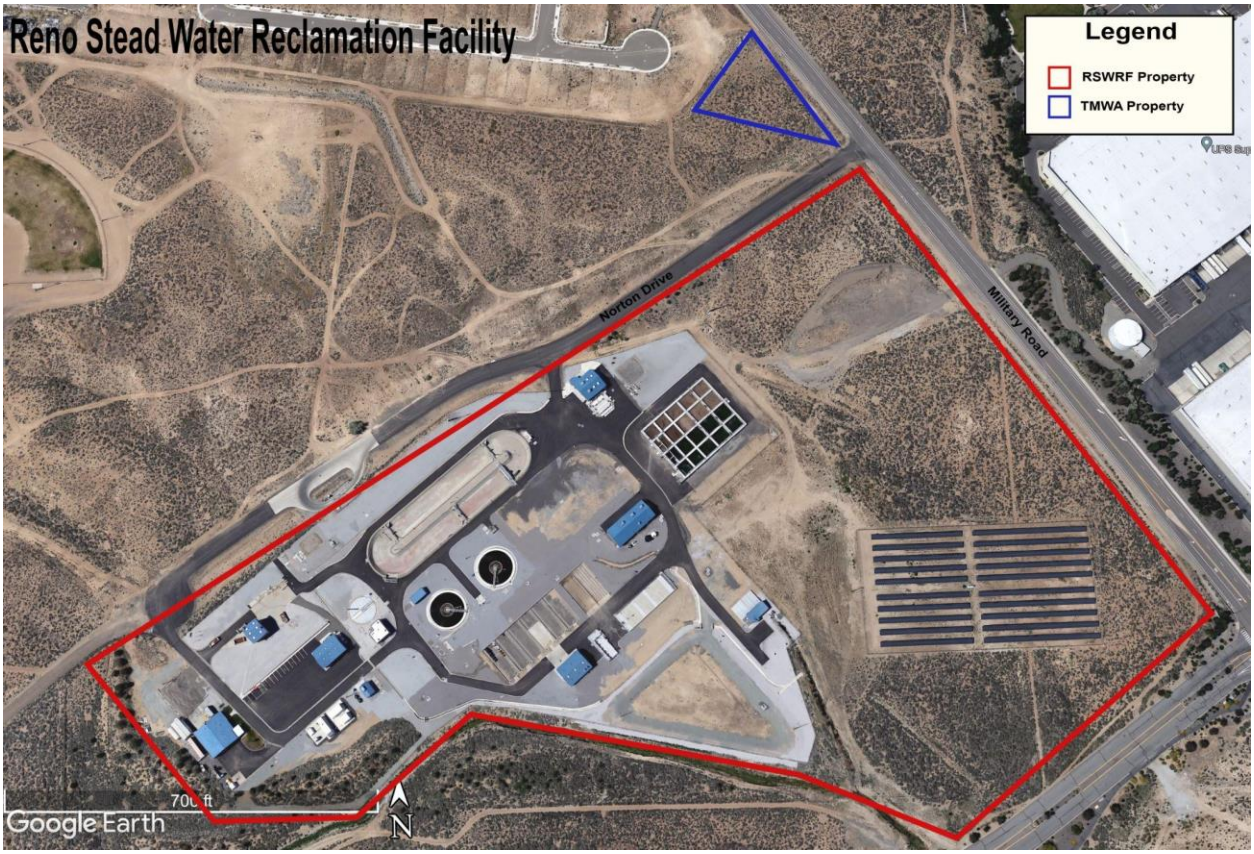

Figure 1.1: Reno-Stead Water Reclamation Facility, Reno NV. Reno-Stead Water Reclamation Facility served as the source of water for the injection test

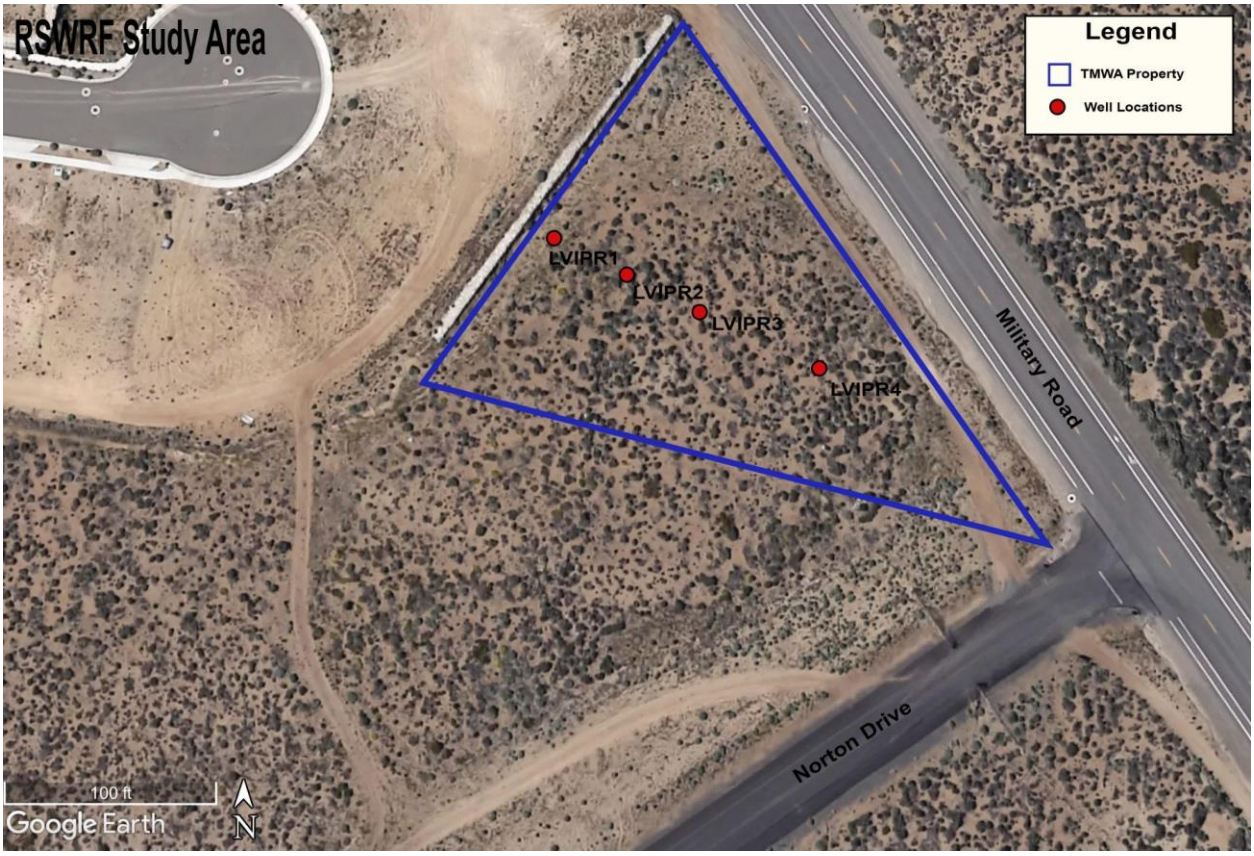

Figure 1.2: Locations of the four wells drilled for the injection test at the Reno-Stead Water Reclamation Facility Study Site. LVIPR1 served as the injection well, LVIPR2 as an intermediate monitoring point and LVIPR3 as an extraction well. LVIPR4 was drilled at a later date in order to collect a soil core and provide a control for temporal arsenic variation observed at the site.

ii. Geologic Description and Well Lithology

The Reno-Stead site sits on an alluvial apron extending from the northern side of Peavine Mountain. Peavine Mountain rises to 8269' amsl to the south of site and consists primarily of faulted granitics with some volcanic influence (Harrill, n.d.). Alluvial aprons in Lemmon Valley are composed of both unconsolidated and semi-consolidated sands, silts and clays with interbedded gravels and cobbles in some locations (Cordy & Szecsody, 1985). These aprons are often overlying relatively shallow uplifted bedrock or semi-consolidated granitic formations (Harrill, n.d.). The Reno-Stead site is located just

south of the Airport Fault which runs to the North-Northeast and separates the valley into the West (92A) and East (92B) hydrologic basins (Cordy & Szecsody, 1985).

Construction of the 4 wells at the site show lithology consisting of fine to coarse-grained soils of silty sand with small lenses containing gravel/fractured rock. Additionally, several lenses of sandy and silty clay were identified. At greater depths In LVIPR1 and LVIPR4, lithology transitions to fractured, weathered granitic rock, potentially indicating a transition zone 100-150' below the site. Well construction and lithology can be seen in Figure 2. Aquifer tests performed at LVIPR1 and LVIPR3 resulted in transmissivities of the aquifer ranging from 56-61 ft^2/day and hydraulic conductivities of 0.6-0.7 ft/day (Pohll *et al.*, 2019).

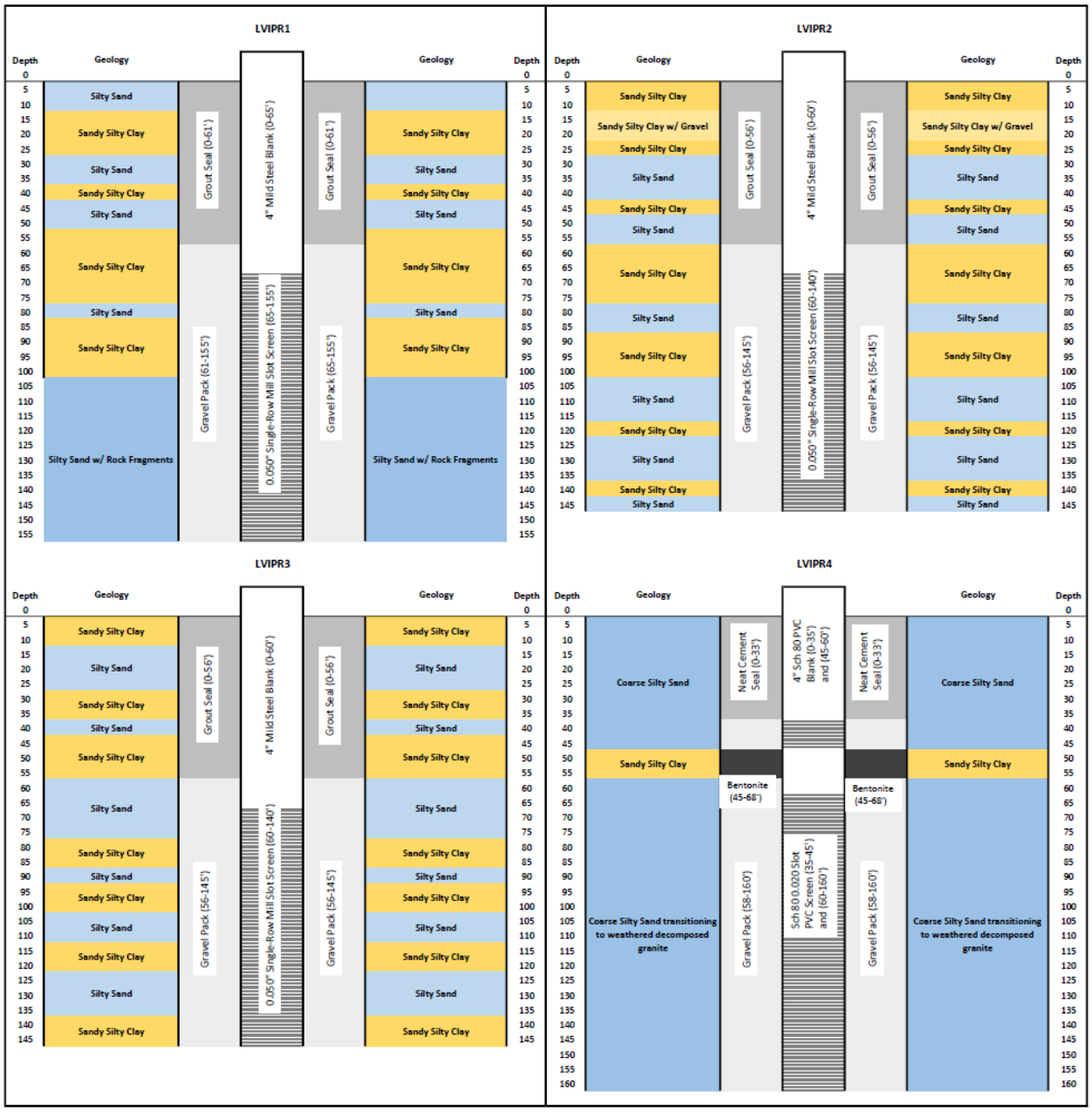

Figure 2: Well construction and Lithology for the four wells constructed at the Reno-Stead Site

b. Need for Work/Motivation

Artificial aquifer injection through the use of potable water and now newly defined and regulated "A+" reclaimed water is becoming increasingly important components of a stable water portfolio for the Northern Nevada, USA region (Drewes *et*

al., 2003). Primary goals of aquifer recharge projects are to improve water sustainability as well as provide additional methods by which to dispose of and store wastewater that otherwise may be lost (Dillon *et al.*, 2006). Because of the need to ultimately utilize artificially injected water in the future, it is important that existing groundwater chemistry and the chemistry of the injected water are compatible, and neither is degraded during injection and storage. A pilot project to determine the feasibility of Indirect Potable Reuse (IPR) and A+ water was implemented at the Reno-Stead Water Reclamation Facility located just north of Reno, Nevada. At this site, natural arsenic levels were observed to be above the MCL (Maximum Contaminant Level) and temporal variability in arsenic concentration was observed during injection tests. Geochemical and groundwater flow modeling identified iron-oxide encrustations on the well casing to be the potential driver of the arsenic variability seen (Perez, 2020). Additional characterization, experimentation and modeling are needed to confirm the sources of arsenic in this system which are causing the elevated levels observed and how future A+ injection may impact arsenic mobilization. The arsenic concentrations and variability observed at the Reno-Stead site is an ideal test bed for developing and testing a geochemical modeling methodology that could be modified and applied to future injection sites. By developing a framework at this pilot site, future geochemical issues can be identified and avoided before large investments are made in IPR infrastructure

c. Arsenic in Groundwater

i. Arsenic Geochemistry

Arsenic is the 47th most abundant naturally occurring element on earth and is found throughout the globe in various forms, either as free arsenic or as part of, or

bonded to, various minerals. It can occur in organic and inorganic forms however organic forms are rarely discussed and are of limited concern as organic arsenic becomes detoxified through methylation during biological processes (Yao *et al.*, 2014). Arsenic does not break down or degrade in the environment. It is cycled through free arsenic into or onto minerals until it is released again. Arsenic is unique compared to other heavy metals as it is readily mobilized in pH values common in natural waters. Arsenic can occur in valence states -3,-1,0.+3 and +5 but in natural waters, it is primarily found in valence states 3 and 5 as As(III), Arsenite (AsO_3), and As(V), Arsenate (AsO_5) (Smedley & Kinniburgh, 2002). Arsenic does not typically make up or substitute into major rock-forming minerals but instead occurs primarily as an anion bonded to metals or as a minor component in some minerals (Vaughan, 2006). It can be a primary contaminant in many groundwater and surface water systems either due to natural degradation and mobilization or direct anthropogenic sources. Concentrations in surface water typically range from 0.013-2.1 ug/L in surface water systems and from 0.5->10 ug/L in groundwater aquifers (Vaughan, 2006). These concentrations are highly variable and dependent on location and local water pH and chemistry. Total values of up to 5000 ug/L have been reported in natural waters, but this is rare and highly localized (Smedley & Kinniburgh, 2002). The typically higher values found in groundwater make arsenic a contaminant of concern in global water systems which are dependent on groundwater extraction (Nickson *et al.*, 2000).

Under the conditions found in most natural waters, arsenic is primarily found as As(III) or As(V). In freshwater systems, As(V) is typically dominant over As(III) although As(III) can become more prevalent in waters experiencing reduced conditions

(Smedley & Kinniburgh, 2002). This separation of species has led to research into the use of arsenic speciation as a proxy for understanding redox conditions in waters. This methodology is difficult to utilize in groundwater systems, as pumping can result in water of different redox conditions being pulled from multiple aquifer zones into the well and mixed before samples are taken. A redox reaction for water that contains Arsenite and Arsenate can be seen below (Jang *et al.*, 2016):

$$H_3AsO_4 + 2H^+ + 2e^- \rightarrow H_3AsO_3 + H_2O \quad E_0 = +0.56\ V \quad \text{(Eq. 1)}$$

The pKa values for arsenic can be seen in Table 1: and help to illustrate the speciation of the element (Jang *et al.*, 2016):

Arsenic Species	pK_{a1}	pK_{a2}	pK_{a3}
H_3AsO_4	2.19	6.94	11.5
H_3AsO_3	9.20	----	

Table 1: pKa Values for As^{3+} and As^{5+} (Jang *et al.*, 2016)

Under reduced conditions, arsenic can become more mobile and create more problems in terms of contamination and transport. Eh and pH are the primary controlling factors of arsenic speciation (Vaughan, 2006). As seen in Figures 3.1 and 3.2 (Smedley & Kinniburgh, 2002), Eh and pH changes can cause many changes in arsenic speciation.

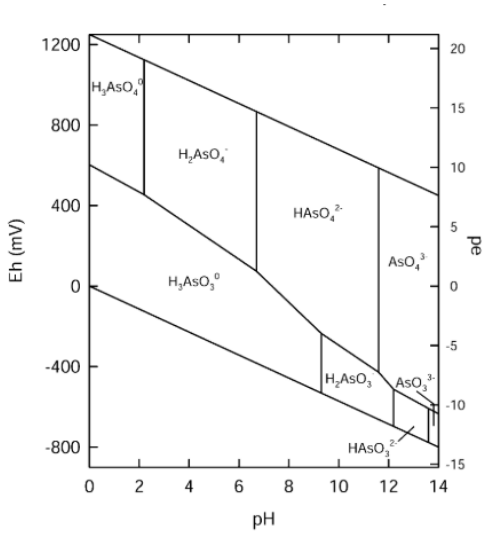

Figure 3.1: Eh-pH diagram for aqueous As species in the system (Smedley & Kinniburgh, 2002).

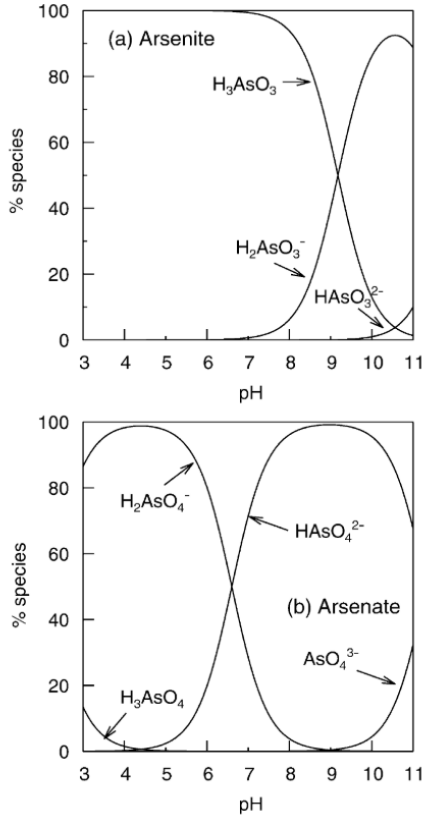

Figure 3.2: (a) Arsenite and (b) arsenate speciation as a function of pH (Smedley & Kinniburgh, 2002).

Under more acidic conditions, arsenic bonds with iron and aluminum if present to some compounds such as $AlAsO_4$ and $FeAsO_4$ while under alkaline conditions, $Ca_3(AsO4)_2$, Calcium Arsenate is the dominate compound (Jang *et al.*, 2016). Under reduced conditions and at pH common in groundwater, arsenic tends to form H_2AsO_3 or Dihydrogen Arsenite. Dihydrogen Arsenite can also be present in oxidized conditions, but only at lower pHs or at low Eh. In oxidized conditions at pH common in natural waters, arsenic tends to form $HAsO_4^{2-}$ Hydrogen Arsenate or $H_2AsO_4^-$ Dihydrogen Arsenate. These species are most common and contribute to the prevalence of As(v) arsenate species found in most waters. Because many of these redox boundaries occur at pH and Eh values that can be achieved in natural waters, arsenic speciation can be highly variable and must be evaluated for each system to determine what species are present and if changing environmental conditions can cause a shift in speciation or mobilization.

Figure 3.2 (Smedley & Kinniburgh, 2002) demonstrates the presence of Arsenite and Arsenate species as a function of pH. For Arsenite, a shift from a solution dominated by H_3AsO_3 (Arsenous Acid) to $H_2AsO_3^-$ (Dihydrogen Arsenite) occurs at a Ph of about 9. $HAsO_3^{2-}$ (Hydrogen Arsenite) starts to occur at a pH of about 10 but at a very small percentage and typically outside the range of natural waters. For Arsenate, 4 species are present in a normal pH range. H_2AsO_4 occurs at a pH of less than 4 and is typically not considered when looking at natural waters. AsO_4^{3-} can also occur, but at pH above 9 and does not start having a significant concentration until pH is above 10 so it is also not typically a concern under normal conditions. Under typical conditions, the shift from $H_2AsO_4^-$ (Dihydrogen Arsenate) to $HAsO_4^{2-}$ (Hydrogen Arsenate) occurs at pH of about 6.5. Arsenate (As(v)) is the most common arsenic state and its speciation shift occurring

at a very neutral pH results in much more speciation occurring in natural waters than other elements.

Because the tendency of arsenic to mobilize and speciate at pH and Eh values common in natural waters, contamination and change in species can occur in areas where previous free arsenic values were low due to changes in redox conditions. The presence of acid rain in some areas is enough to shift pH enough that new arsenic species are formed and different values in water bodies are observed. The rate at which arsenic reacts in solution has not been studied outside of reactions used for analysis and is estimated to be very slow (Ferguson & Gavis, 1972).

Arsenic toxicity to humans is well known and well documented. The oxidation state of arsenic plays a large role in determining the toxicity of the element. Ingestion at the acute level such as drinking highly contaminated water or ingesting pesticides can result in nausea, vomiting, cyanosis, hallucinations and potentially death. Exposure to a smaller level of arsenic over a long period of time can cause chronic issues. This type of exposure is more common and typically caused by ingestion of low-level contaminated water. This type of exposure can cause cardiovascular disease, liver, kidney or bladder disease, or numbness in the extremities (Jang *et al.*, 2016).

Arsenic makes up a large part of over 200 minerals (Smedley & Kinniburgh, 2002). The predominant mineral containing high levels of arsenic is Arsenopyrite (FeAsS) and Arsenian Pyrite ($Fe(SAs)_2$). These minerals are typically formed alongside other ores within the earth and are commonly encountered when mining operations are searching for other ores such as gold. In some instances, mining operations target these

minerals directly as a source of arsenic for industrial purposes. Arsenic is not a major component of rock forming minerals however it is still present at varying levels. Arsenic typically follows the formation of sulfur and usually occurs in sulfides. Arsenic is typically found adsorbed onto minerals rather than being a part of their physical structure. Arsenate adsorbs strongly to iron oxides as well as some clays and calcites to a lesser extent. For this reason, clays typically have higher arsenic loads than that of sands or gravels. Geothermal outflow zones also typically contain elevated concentrations of arsenic among other elements and can be a primary source of groundwater arsenic contamination in areas with high geothermal activity.

Arsenic is produced both intentionally and unintentionally from human-related activities. Historically, arsenic was used in a wide range of products from medicine to poison to metal treatments. Land use from mining, farming or development is currently the primary source of Arsenic release caused by humans (Podgorski *et al.*, 2017). Direct production of arsenic primarily as a pesticide is also a large contributor of arsenic releases worldwide. Most human created arsenic results in localized water contamination in the area immediately surrounding the disturbance, i.e., mining drainage impacting downstream rivers/lakes or arsenic production facilities polluting underlying land or nearby waterways. A large amount of anthropogenic arsenic is also released during fossil fuel combustion and can have far-reaching impacts on water bodies outside of the localized area. It is estimated that for every ton of coal burned for energy production, 2.5 grams of arsenic is released into the atmosphere (Ferguson & Gavis, 1972). This atmospheric deposition can result in arsenic pollution occurring at a much larger spatial scale than localized land use or industrial production. Much of the atmospheric arsenic is

deposited in the area closest to the coal plants with decreasing concentrations as distance from the plant increases, but a significant portion remains in the atmosphere for an unknown amount of time allowing for long-distance stratospheric transportation (Vaughan, 2006). The volume of arsenic released into the atmosphere and water bodies by human causes is much greater than that of natural weathering or deposition. These types of sources are often scattered around the landscape resulting in new point source pollution in addition to natural arsenic deposition.

ii. Arsenic Modeling

Because of the potential sensitivity of minerals such as iron oxides to changes in water chemistry, preliminary modeling before groundwater recharge should be standard. As noted in other studies (Fakhreddine *et al.*, 2015, Gotkowitz *et al.*, 2004, Jones & Pichler, 2007), the sensitivity to pH for these types to minerals makes understanding the equilibrium reactions present in the aquifer prior to injection a key step in the development of an artificial recharge project. Through the collection of relatively simple field parameters and mineral and groundwater samples, the inputs for geochemical models such as PHREEQC can be easily obtained (Sharif *et al.*, 2008). Additionally, short, relatively simple model runs should be completed first to identify potential reactions or minerals that are of higher concern before more full-scale system modeling occurs (Zhu, 2012). The variability in mineralogy between aquifers as well as differences in groundwater chemistry make each model slightly different but overall, every model should follow a similar framework (Wallis *et al.*, 2010). Similar models have been proven to be successful across a variety of aquifer types ranging from

carbonate to silica to alluvial and are able to understand a wide range of mobilization causes (Sharif *et al.*, 2008, Wallis *et al.*, 2011, Zhu, 2012).

A key component in developing an accurate useful geochemical model for evaluating arsenic in an artificial recharge scenario is determining the exact mineralogy of the target aquifer or even the specific zone within the aquifer at which recharge will take place. Collection of representative aquifer minerals should be gathered before or during the drilling of a well and analyzed to determine the composition. X-ray diffraction (XRD), scanning electron microscopic (SEM) analysis or chemical analysis can all be effective, accurate ways to determine mineralogy of the target aquifer (Sharif *et al.*, 2008). Based on determined mineralogy, potential risks of arsenic mobilization can be identified, and model development can be targeted. After potential risks for the target aquifer are identified, the chemistry of injection water can be added to determine if any mobilization occurs. Even properly calibrated, this type of modeling does not guarantee a lack of mobilization at field scale (Sharif *et al.*, 2008, Zhu, 2012). The ability to model a variety of potential injectable water chemistry makes this type of model a valuable tool during recharge program development.

d. Objectives

ASR and IPR are becoming an increasingly considered method of potable water storage and security. A key component in determining the feasibility of these types of projects is understanding the potential changes to aquifer chemistry that may occur during artificial water injection. By fully understanding the mechanisms and geochemistry behind the observed arsenic variability at RSWRF, similar situations can

potentially be identified and avoided at future sites before large investments in infrastructure and time take place. Utilizing the data collected at the Reno-Stead site, the feasibility of a simple geochemical model that can identify interactions between injected water and injected groundwater can be evaluated. The goal of this project is to develop a geochemical model that simulates observed interactions at the Reno-Stead site through replication of batch experiments and measured chemistry changes of both pH and arsenic values. After confirming model accuracy, it can then be used to test potential hypotheses of arsenic release that may explain the elevated arsenic levels observed at the site. This case study in the effectiveness and usefulness of a simple geochemical model will lay the groundwork for potential implementation of this modeling framework at future sites before large investments in both time and money are made.

Previous Work

a. Tracer Study

A 75-day sulfur-hexafluoride (SF6) tracer test was performed at the site to determine travel time between the injection and extraction wells and served as a test before A+ water was injected at the site. Injectate water was saturated with sulfur-hexafluoride gas through a gas mixing system. SF6 gas at a pressure of 25 psi was injected into an in-line ozone mixer in the injectate water pipeline roughly 750ft upstream of the injection well. It is assumed that the water would become saturated with the gas prior to reaching the injectate well and entering the aquifer after entering the mixer and traveling through the injection pipeline. Injection of the SF6 saturated water occurred for 24hrs before the gas injection system was shut-off and “unsaturated” water with no SF6

present continued to be injected for the remainder of the study. Samples of the injectate water were collected at 0hrs, 10hrs, and 23hrs to determine the injected concentration of SF6 present. Daily samples of the extracted water were collected for the remainder of the test. Analysis of SF6 concentration in these samples was performed at the University of California, Santa Barbara via gas spectrometry under guidance of Jordan Clark, Ph.D. Due to the effectiveness of the gas saturation system and the limited dilution that occurred in the aquifer, samples had to be diluted to achieve known values. In this instance, original samples were collected in 1L amber bottles with no headspace. To achieve reasonable SF6 levels, an initial dilution of the samples was performed by opening the bottles and introducing a 10mL headspace directly in the 1L through the removal of 10mL of sampled water and resealing them. The samples were then allowed to equilibrate with the new headspace overnight. The following day, a 1µL sample was extracted from each 1L bottle and placed into a 10mL Vacutainer. The headspace of this Vacutainer was then filled with ultra-high purity nitrogen. At least two samples from each original 1L bottle were prepared in this way. The samples were then allowed to equilibrate for at least 1 hour or up to a day. (No difference between samples was seen between these two equilibrium times.) The final headspace was analyzed via a gas spectrometer. The results of the tracer analysis showed initial concentrations reaching the extraction well at day 4 and a mean arrival time of 33 days. The extraction well was shut down after 95 percent recovery of the tracer occurred 282 days later. The speed at which recharge water was able to reach the extraction well indicates a highly transmissive aquifer and confirms that recharge water is traveling between the injection well and the extraction well.

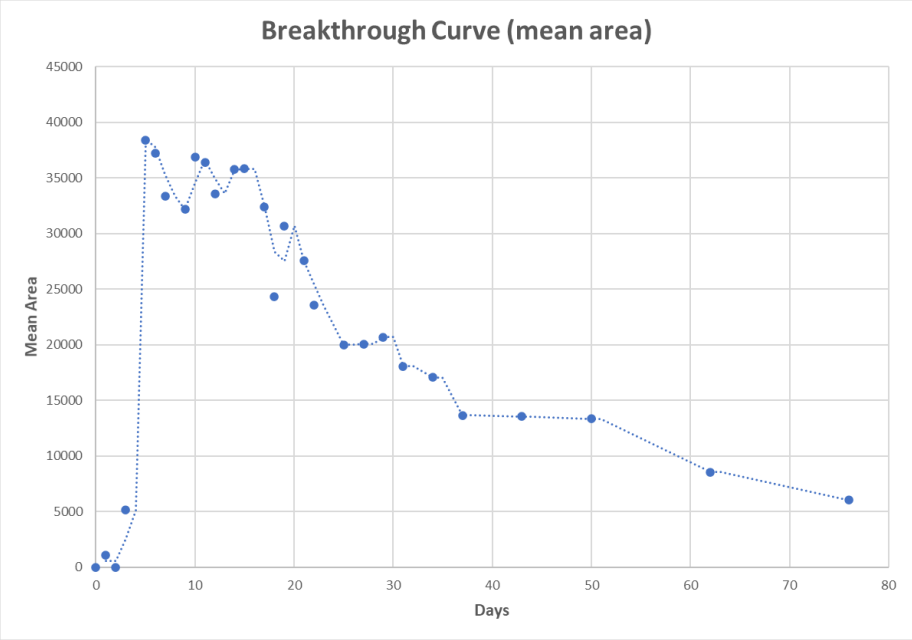

Figure 4: SF6 tracer breakthrough curve. Mean area of the GC curve is used as it shows relative concentration over time.

b. Arsenic Temporal Variation

In addition to tracer samples, water quality samples were collected for a suite of unregulated and regulated constituents before, during and after the tracer test and showed that all constituents except for arsenic were within drinking water standards. Pre-test, arsenic variability was found to be between 0.018-0.022mg/L while post-test levels were between 0.034-0.040mg/L (Figure 5). The change in arsenic levels occurring in the extraction well prompted additional arsenic sampling of injectate water for the final two months of injection. It is expected that as injected water with a much lower arsenic concentration (roughly 0.005 mg/L) is introduced to the aquifer that concentrations at the extraction well would decrease with time unless mobilization is occurring. The maintained higher concentration observed in the extraction well indicates the potential for an arsenic source releasing arsenic into the groundwater throughout testing or the

assumed background concentrations were inaccurate due to inadequate flushing of the well prior to sample to collection.

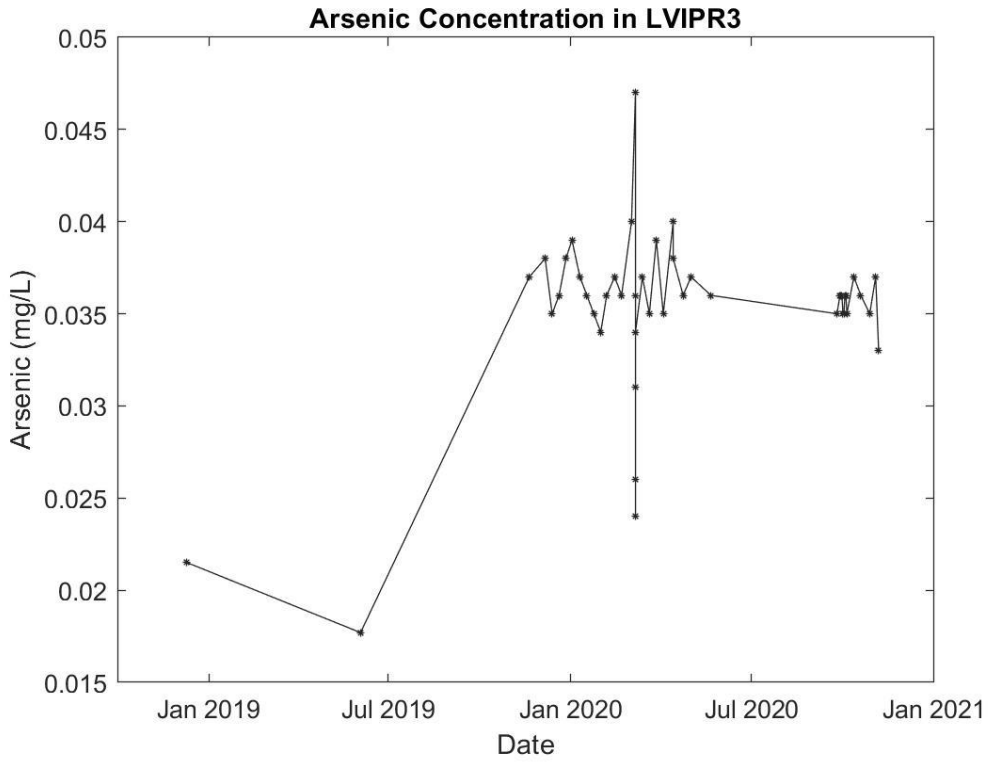

Figure 5: Arsenic concentration in LVIPR3 including pre-injection measurements as well as during injection measurements.

To determine the accuracy of the original background samples, injection and extraction was shut off and water levels were allowed to return to equilibrium. The extraction well (LVIPR3) was then turned on at a rate of ~8gpm, and arsenic samples were collected at startup, 10mins, 30mins, 1hr, 4hrs and 8hrs after startup. The observed arsenic values can be seen below in Table 2.

LVIPR3 Startup Test	
Time	As (mg/L)
Startup	0.047
10min	0.024
30min	0.026
1hr	0.031
4hr	0.036
8hr	0.034

Table 2: Arsenic concentrations at the extraction well (LVIPR3) without injection after aquifer has reached equilibrium.

At startup, arsenic concentrations are higher than "equilibrium" values observed during injection. This is attributed to higher sediment load during startup that may contain sorbed arsenic. At 10 mins, arsenic is 24ppb, similar to the assumed background values collected in 2018 and 2019. As the extraction well continues to run, arsenic values begin to increase until they return to the "equilibrium" level of roughly 34-40 ppb. It was hypothesized that the change in arsenic concentrations at the well head may be due to three potential mechanisms (White & Pohll, 2020). First, desorption of arsenic from iron-oxide minerals in the aquifer results in higher arsenic concentrations than background. Second, sorption of arsenic to iron-oxides that have formed on the mild steel well casing reduces concentrations at early time sampling. Third, arsenic concentrations are naturally higher at depth and drawdown during pumping results in greater concentrations to enter the well as dilution with the upper aquifer zone is reduced. Construction of LVIPR4 was completed utilizing PVC to eliminate the possible effects of hypothesis 2 and the well was screened in such a way as to facilitate isolated sampling of the well in an upper and lower zone. Ultimately, sampling of the well resulted in a composite concentration of 0.036mg/L and only minor observed differences between the upper and lower aquifer zones. Based on these results, it was determined that sorption to iron-oxides present on

the mild steel casing of LVIPR3 resulted in the arsenic variation seen at startup. Upon startup, arsenic concentrations in the well and immediately surrounding the well are artificially low due to removal by sorption to the well casing. At later times, this “bubble” of low concentration water is removed and water from the surrounding aquifer enters the well at the background concentrations of 0.034-0.040mg/L. This is a common occurrence in wells constructed with a mild steel casing and can result in artificially low arsenic concentrations if the well is sampled too early before proper purging has taken place (Hinkle & Polette, 1999). This result also led to the assumption that the previous “background” samples collected in 2018 and 2019 were had artificially low arsenic concentrations due to sample collection near startup. The new background concentration is assumed to be in the 0.034-0.040mg/L range observed during testing (White & Pohll, 2020).

While the effects of iron oxides on the well casing explain the variability of arsenic scene over the short-term, there is still the expectation that over the long-term with injection occurring the background concentration would be reduced as it is diluted with injection water of low concentration. The near constant, high concentration observed during the injection test indicates that there is another mechanism for arsenic release occurring in the aquifer itself.

Methodology

a. Mineralogy

    i. X-Ray Diffraction (XRD) and X-Ray Fluorescence (XRF) Analysis

The soil core that was collected during the drilling of LVIPR4 was utilized to determine the exact mineralogy and elemental composition of the aquifer. Each collected 10’ core section was dried at 40 degrees Celsius for 24 hours, crushed and sieved to 0.5mm before being sent for X-Ray Diffraction (XRD) and X-Ray Fluorescence (XRF) analysis by DRI (Perez, 2020). XRD analysis of the soil core was conducted by Tex-Ray Laboratory Services in Argyle, Texas. The observed mineralogy as well as relative abundance reported was used to create the simulated aquifer mineralogy that will be used in the PHREEQC conceptual model.

ii. Scanning Electron Microscopy (SEM) Analysis

In addition to XRD analysis, portions of the crushed and sieved soil core were analyzed utilizing a scanning electron microscope to better understand mineral morphology as well as elemental composition. SEM analysis was performed utilizing a Hitachi TM-1000 table-top microscope paired with a SwiftED-TM EDX spectrometer located at DRI. For this analysis, a representative core segment was chosen to analyze. The core containing sediment from 91-101’ below ground surface was chosen as it was fairly representative of the entire core and captured the zone where elevated arsenic was observed. The core sample was then analyzed at three different magnifications, 40X, 500X and 1000X. Results of this analysis will be used to verify the results of the XRD and XRF analysis as well as help identify the structure of the minerals.

b. Batch Experiments

i. Experiment Setup

In order to better understand the mechanism behind the nearly constant "equilibrium" arsenic concentrations despite the injection of lower concentration water, batch experiments were performed by Lazaro Perez, Ph.D. and Ron Hershey, Ph.D. of Desert Research Institute. Aquifer material was obtained for the batch experiments from the soil core collected during the drilling of LVIPR4. This was the same core that was also used for XRD and SEM analysis. The goal of these batch experiments was to better understand any changes in pH that occurred when the synthetic water of varying initial pH interacted with the aquifer mineralogy. Additionally, "spiked" arsenic solutions were created to determine how the mineralogy reacted at the varying pH values.

ii. Parameters

A "spiked" arsenic solution was created by dissolving 4.15g of Na2HAsO4 in 100mL of high purity water. 10mL of this solution is then added to 1L of high purity water to create a solution containing 1.33×10^{-3} M As. To adjust the pH of the synthetic groundwater either 1.6 N sulfuric acid (H2SO4) or 0.1 N sodium hydroxide (NaOH) to reach the desired pH. pH solutions of 6.5, 7.0, 7.5, 8.0 and 8.5 were created for this experiment. (Perez, 2020). The batch experiments were conducted utilizing 15mL polystyrene test tubes containing 10mg of the 0.5mm sieved core material, 15mL of each of the pH adjusted synthetic groundwater. The test tubes were then centrifuged at 3000 rpm for 30 minutes and then stored for 32 hours before final pH was measured and fluid was collected, filtered to 0.45 mm and submitted for arsenic analysis.

c. PHREEQC Modeling

i. Model Setup

The geochemical modeling conducted for this study utilized the PHREEQC version 3 software developed by the United States Geological Survey (Parkhurst & Appelo, 2013). The developed model consisted of a "Base Model" and a "Surface" model. The base model was developed to verify the accuracy of the model mineralogy with that of the observed mineralogy from the Reno-Stead site. The Wateq4f (Ball & Nordstrom, 1991) database was chosen for this model as it allowed for surface complexation reactions utilizing the Diffuse Layer Model developed by (Dzombak & Morel, 1990) that will be needed for the iron-oxide sorption model. Additions and modifications to the Wateq4f database were made as needed to include relevant mineralogy and surface reactions. The base model mineralogy was taken from the observed mineralogy that was reported from the XRD analysis. The results of the XRD analysis were reported in weight percentages of the present minerals. Because this model was created to initially replicate the results from the batch experiments in which 10mg of sediment was utilized, the report weight percentages were converted to theoretical weight of each mineral present in 10mg of soil core. The weight percentages of each 10ft soil core were reported but for this study, an average was taken and used for the model. After determining the theoretical weight present in an average of 10mg of soil core, the mineral weights were then converted to the number of moles present in 10mg of soil for use in the PHREEQC model input. The synthetic water used in the batch experiments was also simulated for the model. The simulated synthetic water was assumed to contain negligible amounts of cations/anions present and only pH, pe, temperature and alkalinity were modeled.

ii. Batch Experiment pH Replication

Before testing the Iron Oxide Hypothesis , the model was validated by comparing pH changes observed during the batch experiments with modeled pH changes after the simulated synthetic water was allowed to equilibrate with the mineralogy entered into the model based on the XRD analysis. For this model run, no arsenic concentration was included in the model. The model was run for pH values matching those tested in the laboratory batch experiments (6.5, 7, 7.5, 8 and 8.5). Each model run utilized the same base model with the only change occurring being that of pH. Each model run then equilibrated the simulated synthetic water with the mineralogy of the Reno-Stead site and the resulting pH values were then compared to those measured during the laboratory batch experiments. Accuracy between the model runs and that results from the batch experiments validate the mineralogy present in the model before testing the two hypotheses.

Accuracy of the model and goodness of fit between the modeled and laboratory experiments was determined via root mean square error:(Hafeznezami *et al.*, 2016).

$$RMSE = \sqrt{\frac{\sum_{i=1}^{N} (Predicted_i - Actual_i)^2}{N}}$$

For this metric, predicted values are the modeled final pH values and actual values are the pH values from the laboratory experiments. N corresponds to the number of data points, in this instance 5, one for each of the initial pH values.

During the batch experiments, a small amount of headspace was present in the vials along with the synthetic groundwater and native soil. Having air present in the headspace during the batch experiments could have resulted in skewed final pH values as the synthetic water not only interacted with the soil but also with the small amount of air present in the vial. When carbon dioxide dissolves in water the formation and eventual dissolution of carbonic acid results in an increase in H_3O^+ ions and corresponding decrease in pH. The opposite effect is true under increased oxygen concentrations, pH is likely to increase in response to a reduction in H^+ ions. The created PHREEQC base model did not contain headspace and was run assuming the only interactions occurring were between the water and soil. After running this model, it was noted that the small amount of headspace present in the vials during the batch experiments likely did impact pH. To accurately validate the model, the base model was modified to include a small amount of "air" that would also interact with the synthetic water. It was assumed that 1ml of air was present in the vials during the experiments. The only components of standard atmospheric air that were assumed to potentially impact pH were oxygen and carbon dioxide gas and these were the only two added to the model.

iii. Iron Oxide Hypothesis

The first hypothesis to be tested with this model is the Iron Oxide Hypothesis. In this scenario, sorption and subsequent desorption is hypothesized to be the "source" of arsenic at the Reno-Stead site. Although field samples indicate the presence of free arsenic in the groundwater at the site, the continued elevated arsenic values observed during the injection of "clean" water indicates a source of arsenic at the site. A potential source of this arsenic is through free arsenic sorption to Iron-Oxides present in the

mineralogy of the aquifer. Sorption of arsenic to Iron-Oxides is well documented (Ahmad & Bhattacharya, 2019, Robinson *et al.*, 2011, Welch & Lico, 1998) and is thought to be a primary source of arsenic in areas where arsenic levels are elevated and no anthropogenic or arsenic bearing minerals are present (Hafeznezami *et al.*, 2016). The laboratory batch experiments demonstrated that the mineralogy samples from the Reno-Stead site were able to remove arsenic from artificially "spiked" synthetic water that was added to the soil. This supports the hypothesis that iron-oxides are present at the site. The degree to which arsenic was able to be removed by the soil is dependent on the initial pH of the synthetic water. The pH dependence of soils ability to remove arsenic provides additional support to the iron-oxide hypothesis. Arsenic sorption to iron-oxides was identified as the mechanism by which arsenic variation was observed at short times in LVIPR3. The variability observed over short times at LVIPR3 was likely caused by iron-oxide buildup on the steel well casing itself and not naturally forming iron-oxides in the surrounding aquifer.

To create the PHREEQC model for the Iron-Oxide hypothesis, the base model developed during the batch experiment replication was modified through the addition of reactive iron-oxide surfaces for use in a diffuse layer model developed by (Dzombak & Morel, 1990) that is run through PHREEEQC. Surface site values for iron are typically in the range of 1-5% by weight (Mosier *et al.*, 1991). A weight percentage for iron of 3% was chosen and following the methods described in (Parkhurst & Appelo, 2013) and the ratio of 0.2 weak sites and 0.05 strong sites per mol of iron oxide (Dzombak & Morel, 1990), 7.16E-5 weak sites and 2.69E-7 strong sites of iron-oxide were added to the model for arsenic sorption. In addition to adding the iron-oxide surfaces to the model, the

surfaces were equilibrated with the native groundwater conditions that are present at the Reno-Stead site including an average background groundwater arsenic value of 0.037 mg/L (Pohll *et al.*, 2019). All other background conditions were taken from a sample collected June 3, 2019 (Pohll *et al.*, 2019). This equilibration was done to generate a surface that had an accurate number of available surface sites available when the simulated "spiked" synthetic water was introduced. Because the spiked water contains a higher concentration of arsenic than that of the water the surface was equilibrated with, it is assumed that arsenic reduction will occur if iron-oxides are in fact the mechanism of arsenic sequestration in the mineralogy.

After generating an iron-oxide surface that has been equilibrated with simulated groundwater conditions, the simulated "spiked" synthetic water containing the same 1.33e-6 molar arsenic concentrations as the laboratory experiments was allowed to reach equilibrium with the same mineralogy developed in during the pH replication experiments and with the iron-oxide surfaces. The initial pH was adjusted utilizing the same range (6.5 ,7 ,7.5 ,8 ,8.5) as the batch experiments as well as initial pH values of 6 and 9 to help visualize the full arsenic sorption curve. The modeled final arsenic concentration was then taken and compared to that of the batch experiments to determine if the iron-oxide surface was able to replicate the overall arsenic concentration reduction that was observed during the laboratory experiments. Although real-world conditions in the aquifer would be anaerobic, this model scenario was run utilizing the same headspace addition as the batch experiments. The addition of the headspace is necessary for the modeled results to be an accurate comparison with the results of the batch experiments.

iv. Aquifer Condition Simulation

In addition to exploring the impacts of iron-oxides on arsenic reduction at the Reno-Stead site, the developed PHREEQC model was also used to help explain the apparent arsenic mobilization that was occurring during injection. To simulate conditions similar to that in the aquifer, the same iron-oxide surface complexation values and mineralogy that was used in the laboratory replication models were utilized here as well. CO_2 and O_2 were not included in this model as it is assumed that the aquifer is anoxic. Injected water was simulated by utilizing the water quality results from an injection sample collected June 3, 2019 (Pohll *et al.*, 2019). This background sample contained an arsenic concentration of 0.0023 mg/l. In order to allow the model to react and reach an equilibrium at a larger scale, the model was scaled up from the batch experiments. The amount of mineralogy present in the model was increased by 2 orders of magnitude to better replicate the abundance of reactive mineralogy relative to water at the site. This scaling does not result in a model that is perfectly reflective of the ratio of groundwater to aquifer media at the Reno-Stead site but will allow for a general insight into the trends of the reactions occurring at a larger scale.

To create a simplified representation of the interactions between injected water, native groundwater and the aquifer mineralogy, this simplified "aquifer" model was run by first mixing the simulated injected water and the native groundwater and then having the mixed solution reach a new equilibrium with the mineralogy and surface-sites developed in the previous two models. For this model, the mixing ratio of the simulated injected water and native groundwater was considered to be 80% injected water and 20% native groundwater as determined by flow modeling (Pohll *et al.*, 2019). It is assumed

that the injected water is displacing the native groundwater over the majority of the study site, however some mixing can and will occur with the native groundwater. The surface complexation sites were also in equilibrium with the native groundwater before the mixing and re-equilibration of the mixed solution with the sites. As with the arsenic sorption model, this model was run 7 times, each with a different initial pH value (6 ,6.5 ,7 ,7.5 ,8 ,8.5 ,9) and the results of the model were compared to determine the impact that the different pH values had on the amount of arsenic in the final solution. A second version of this model was run without any iron-oxide surfaces present. This version will allow for a comparison between the surface and no-surface models to further validate that iron-oxides are the primary mechanism of arsenic variability. This model is a simplified interpretation of the conditions occurring in the aquifer and does not take into account the entirety of the geochemical reactions that are occurring at the site. This model is not intended to fully replicate the field observations at the site but instead will help better understand the behavior of potential arsenic release.

Results

a. X-Ray Diffraction (XRD) and X-Ray Fluorescence (XRF)

The lithology and weight percentages of rock forming minerals of 5 of the cores are shown in Table 3.1. Based on the measured mineralogy and their relative abundance, the lithology at the site can be classified as granodiorite-quartz monzodiorite (Perez, 2020).

XRD Minerology					
Core Depth >>> Mineral	35-45	65-75	91-101	115-125	141-151
Albite	35.3	27.2	29.2	43.8	40.1
Quartz	16.3	15	11.7	11.4	20.5
Anorthite	13.1	8.1	9.9	0	0
Muscovite	12.9	18.7	22.5	13.9	11.5
Microcline	11.5	7.2	11.8	14.1	12.1
Gismondine	4.8	2.5	3.4	7.9	2.5
Sanidine	4	0	0	0	0
Cordierite	1.4	0	2.2	1.4	1.8
Richterite	0.8	3.4	3.4	1.3	0.5
Tremolite	0	3.4	0	0.9	0
Phlogopite	0	2.7	0	0	0
Kaolinite	0	2.1	3	0.9	1.2
Montmorillonite	0	1.1	1.1	2.4	1.7
Diopside	0	0.6	0	0	0
Feldspathoid	0	0.5	0	0	0
Dolomite	0	0	0.6	0.1	2.8
Lime	0	0	0.3	0	0
Pyrophyllite	0	0	0	1.9	0
Gehlenite	0	0	0	1.1	0

Table 3.1: Weight percentages of rock forming minerals found in the aquifer. Columns indicate soil core depth in feet.

Major oxides present in the aquifer are presented in Table 3.2. Silica is the dominant oxide in this aquifer system. Based on the composition and relative abundance of these oxides, the predominant rock into which this well is drilled was identified as granodiorite (Perez, 2020). The presence of iron oxide in the aquifer is expected in a granitic system and supports the hypothesis that iron-oxide sorption plays a role in potential arsenic sorption or mobility (Appelo & de Vet, 2003, Currell *et al.*, 2011). Table 3.3 provides minor elements found in the aquifer. Arsenic is present throughout the core with higher concentrations relative to the total core average found near the surface and from 90-130’ below ground surface.

XRF Major Oxides					
Core Depth >>> / Chemical Formula	35-45	65-75	91-101	115-125	141-151
AL2O3	18.20	18.59	18.78	18.50	18.07
SiO2	65.36	65.06	66.37	65.78	67.71
TiO2	0.84	0.89	0.84	0.86	0.78
Fe2O3	6.35	6.97	6.41	6.64	5.71
MnO	0.10	0.11	0.10	0.11	0.08
MgO	2.13	2.40	1.87	2.47	1.42
CaO	4.01	3.92	3.95	4.15	3.97
Na2O	6.08	3.48	3.98	3.75	4.26
K2O	1.97	1.79	1.74	1.91	1.71
P2O5	0.23	0.23	0.20	0.24	0.17
SiO2	0.03	0.01	0.01	0.01	0.01
CL	0.31	0.00	0.02	0.02	0.02
LOI	3.58	4.72	3.81	3.80	2.77

Table 3.2: Weight percentages of major oxides found in the aquifer.

XRD Minor Elements					
Core Depth >>> / Chemical Formula	35-45	65-75	91-101	115-125	141-151
As	10.1	2.3	10.9	12.8	2.3
Ba	757.1	739.7	705.2	736.2	724
Br	19944.8	18197.5	20678	0.86	21563.6
Cd	0.1	0.2	0.1	0.2	0.1
Co	23.5	24.8	23.5	27.8	9.3
Cr	38.4	40	42.2	42.7	35.5
Cs	0	0	3.95	0	0
Cu	230.9	146.5	111.2	134.1	61.9
Ga	17.5	19.1	22.3	21.2	20.7
Hf	4.7	8.8	2.5	6.9	7
Hg	0.1	0.1	0.1	0.1	0.1
La	36.8	36.9	37.9	38.7	37
Nb	6.2	4.2	6.5	8.1	6.4
Ni	27.5	25.5	26.2	28.1	19.6
Pb	13.1	13.4	16.6	17.8	13.7
Rb	52.7	53.9	50.7	57.1	42.9
Sc	16.4	14.7	16	15.4	4.9
Sn	4.8	4.5	4.3	4.5	3.3
Sr	538.5	509.4	551.8	545.8	590
Th	9.5	10	8.8	6.7	7.5
U	1.7	1.6	1.8	1.9	1.8
V	134.8	139.1	140.6	124.9	128
W	2	2.34	2.4	2.7	2.5
Y	19.7	20.8	20	21.1	18.3
Zn	104.9	103.7	90	99.1	68.7
Zr	215.1	240.8	244	194.4	217.9

Table 3.3: Minor elements present in the aquifer. Units are in parts per million.

b. Scanning Electron Microscopy (SEM)

Analysis of the SEM data further supported the results of the XRD analysis. All three magnifications indicate that silicon is the primary element in the aquifer at this depth. Aluminum and iron are also common and fairly abundant through all three images. There is an observed correlation between relative iron abundance and the amount of arsenic observed in each image. This further supports the hypothesis that arsenic may be sorbed to iron oxide minerals in the formation. At 500x and 1000x magnifications, a reflective surface is observed and shows up in the microscope imagery as a white colored face on the particles. The larger particles appear to be covered in smaller, almost flat particulates that are likely clay/silt minerals. The different spectra can be seen in Figure 6.1-6.3 respectively.

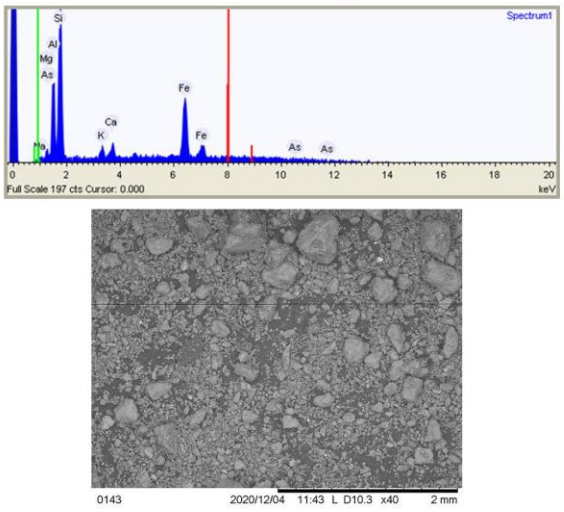

Element	Weight %
Sodium	1.6
Magnesium	2.4
Aluminum	19.2
Silicon	39
Potassium	2.1
Calcium	2.6
Iron	30.8
Arsenic	2.3

Figure 6.1: 40X Magnification EDX Scan Spectra and image for core sample 91-100’ below ground surface.

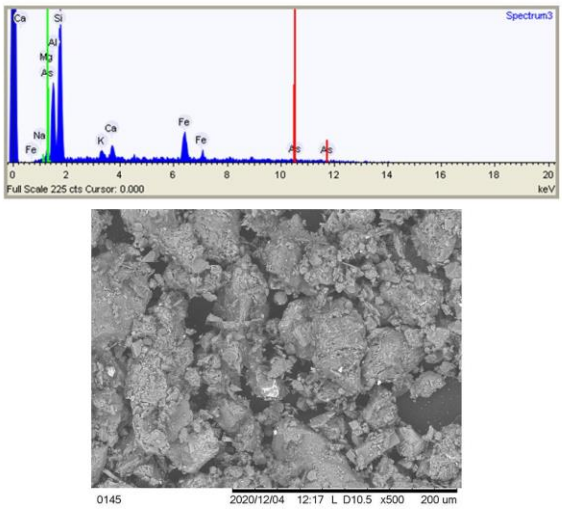

Element	Weight %
Sodium	0.9
Magnesium	2.9
Aluminum	21.5
Silicon	47.1
Potassium	2
Calcium	4
Iron	20.4
Arsenic	1.3

Figure 6.2: 500X Magnification EDX Scan Spectra and image for core sample 91-100’ below ground surface.

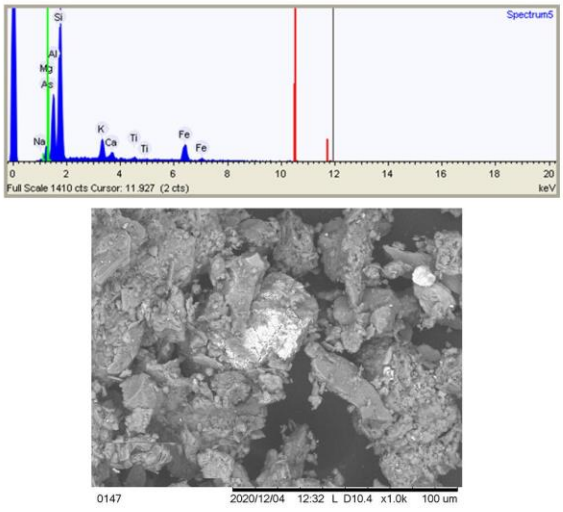

Element	Weight %
Sodium	0.6
Magnesium	7.3
Aluminum	18.6
Silicon	50
Potassium	6.4
Calcium	2.3
Titanium	0.9
Iron	13.3
Arsenic	0.7

Figure 6.3: 1000X Magnification EDX Scan Spectra and image for core sample 91-100’ below ground surface.

c. Batch Experiments

For each initial pH (6.5, 7.0, 7.5, 8.0, 8.5), the final pH and arsenic concentration after centrifuging were measured. The results are broken into two figures seen below.

Final pH relative to initial pH can be seen in Table 4 and the amount of Arsenic that is adsorbed relative to the initial concentration can be seen in Figure 7.

Initial pH	Final pH	Percent Increase
6.5	6.56	1%
7	7.12	2%
7.5	7.53	0%
8	7.93	-1%
8.5	8.51	0%

Table 4: pH change from initial solution after reaching equilibrium with aquifer mineralogy.

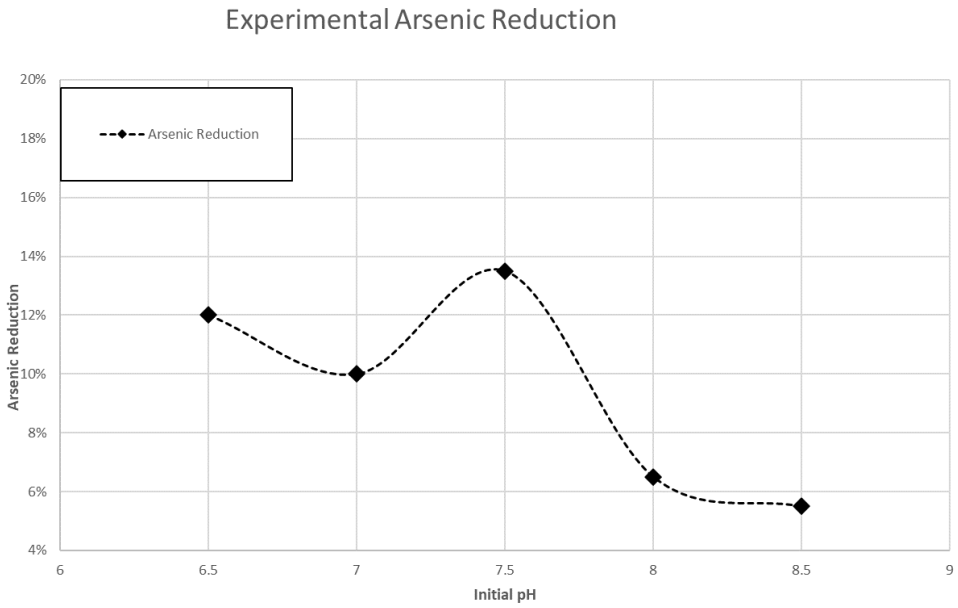

Figure 7: Observed arsenic reduction capacity of the aquifer mineralogy during the batch experiments.

For pH values on 6.5,7,7.5 and 8.5, a small increase in final pH was observed after equilibrium with the aquifer mineralogy. For the initial pH of 8, a small decrease of less than 1% was observed. In the arsenic removal tests, the greatest amount of arsenic removal occurred at an initial pH of 7.5 with a 13.5% reduction of arsenic concentration

observed. The least amount of arsenic reduction occurs at a pH of 6.5. The observed reduction in arsenic further supports the hypothesis that the mineralogy has the ability to sorb arsenic likely caused by iron oxides. This is supported by the observed correlation between iron and arsenic from the SEM analysis. Iron oxides are dissolved at stronger acidic and alkaline conditions resulting in the release of arsenic ((Raven *et al.*, 1998, Stollenwerk *et al.*, 2007). Under more neutral pH conditions, iron oxides are stable and are able to maintain sorbed arsenic or potentially remove arsenic if all sorption sites are not occupied.

d. PHREEQC Modeling

i. Batch Experiment Replication

Two validation models were run to replicate the results observed in the batch experiments, one without any headspace present and one with headspace present. The initial model validation run did not include any headspace. At a pH of 6.5 and 7, the lack of headspace did not result in a significant difference between the modeled and experimental pH. However, at a pH over 7, the modeled pH and experimental pH began to drift apart significantly. At these higher pH values, the model was not able to be validated when compared to the observed experimental pH. The RMSE for this model is 0.871. These results can be seen in figure 8.

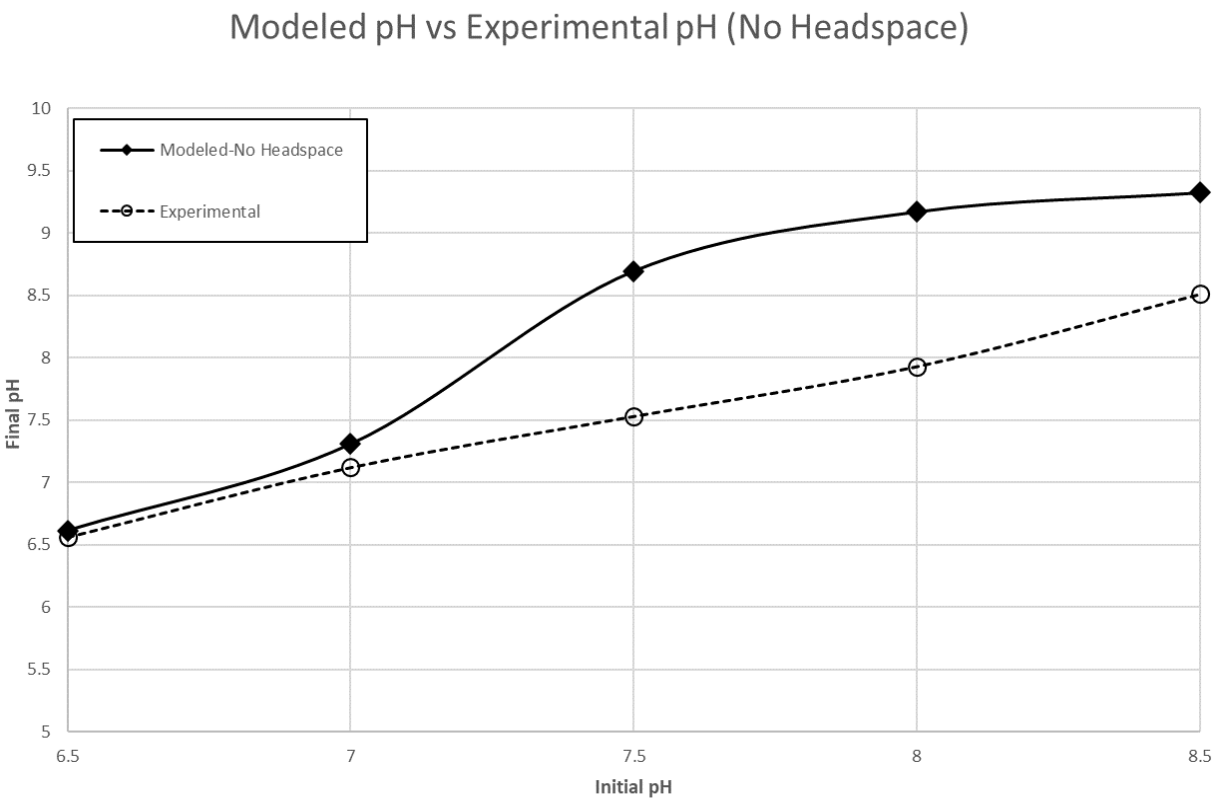

Figure 8: Modeled final pH after reaching equilibrium with aquifer mineralogy for different initial pH values compared to experimental results. No headspace was included in the model.

When the base model was modified to include a small amount of headspace, model performance improved significantly. Error between observed and modeled values improved at all initial pH values tested with the highest error still observed at pH values above 7. The RMSE for this model run was 0.126. This indicates that the headspace present in the batch experiments was a likely source of error in the original model run. This headspace was not exact and may have varied between data points. Despite this source of potential error, the modified base model with headspace replicated the experimental results without significant error. Because the addition of the headspace to

the model was all that was needed to replicate the experimental results, the geologic principles and mineralogy included in the model were deemed accurate.

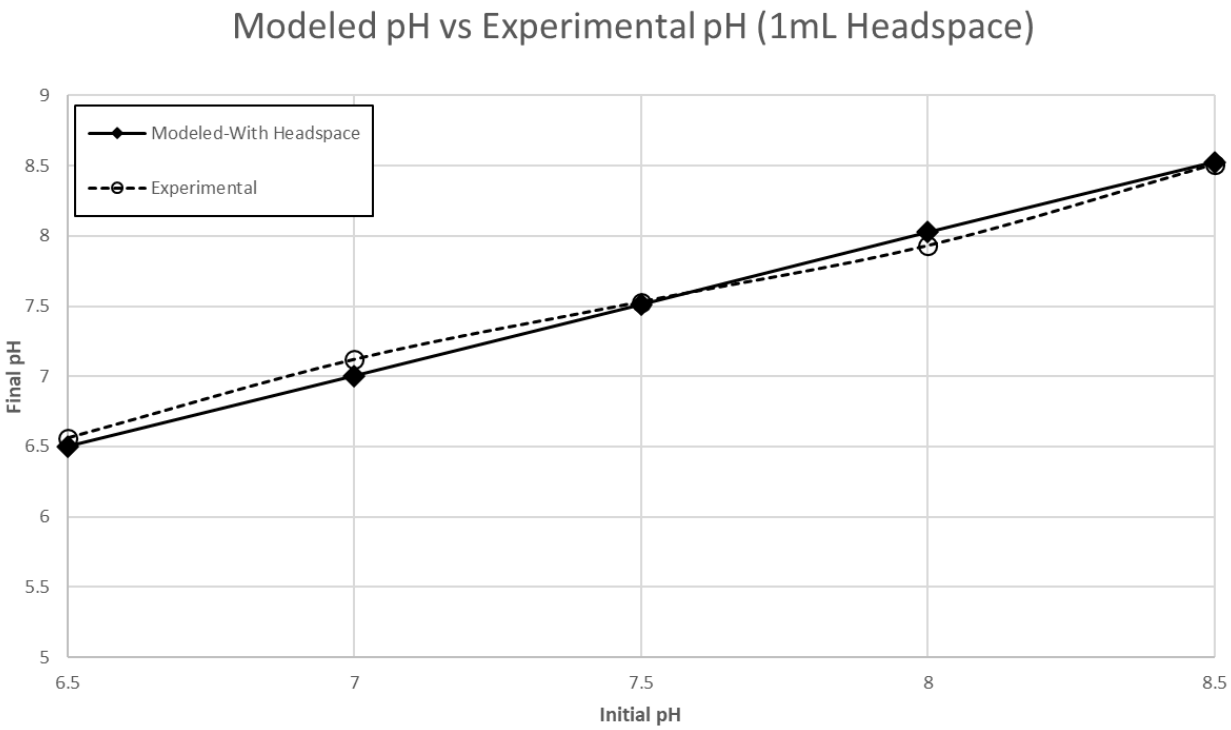

Figure 9: Modeled final pH after reaching equilibrium with aquifer mineralogy for different initial pH values compared to experimental results. Headspace was included in the model.

ii. Iron Oxide Hypothesis

After validating the model through the batch experiment pH replication, the model was then run to determine if the addition of iron-oxide surfaces simulated the same arsenic reduction that was observed in the batch experiments. The results of this model run in comparison to the batch experiments can be seen in Figure 10. As was the case in the batch experiments, the greatest amount of arsenic reduction occurred at a pH of 7.5 with a 15% reduction in arsenic concentration observed. A 14% reduction in arsenic concentration at a pH of 7.5 was observed in the batch experiments. Arsenic reduction

decreased at both more acidic and more basic pH values with the least amount of arsenic reduction occurring at a pH of 9 with only a 1% decrease observed. This decrease in arsenic removal capacity as pH values move away from neutral is attributed to a decrease in iron-oxide surfaces' ability to adsorb arsenic at these pH values. This reduction in sorption capacity can be attributed to the release of arsenic in aquifer conditions (Masue *et al.*, 2007). Even small shifts in pH values can have a large impact on this mineralogy's ability to capture or release arsenic and supports the hypothesis that introduction of injected water with a different pH than the native groundwater at the Reno-Stead site may be responsible for the continued elevated arsenic levels that were observed.

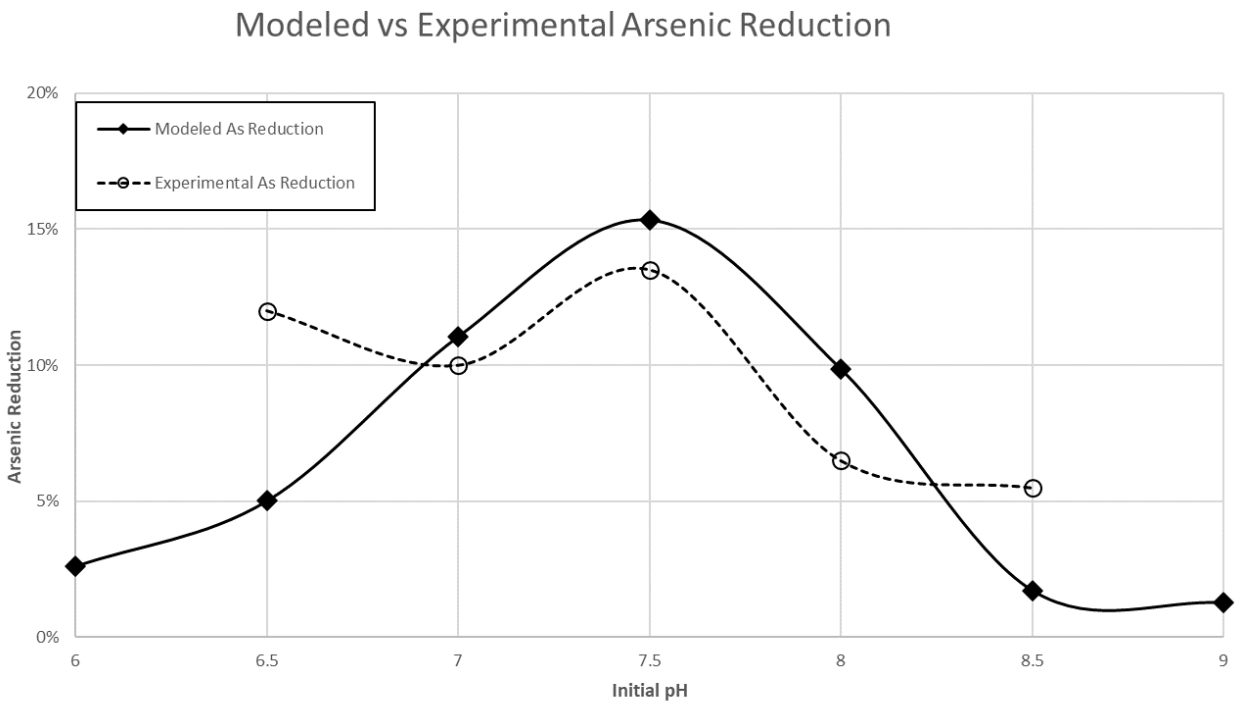

Figure 10: Modeled arsenic sorption capacity represented by percent arsenic reduction from an initial concentration of $1.33E^{-6}$ mol/L compared with the observed sorption capacity with the same initial arsenic concentration during batch experimentation.

Comparing the modeled results to the batch experiment results shows a similar overall trend in arsenic reduction capacity however the model and the batch experiments begin to diverge at the more basic and acidic pH values. The batch experiments show higher arsenic reduction capacities than the modeled results at pH values on 6.5 and 8.5. This divergence between the modeled and laboratory results may be caused by a secondary arsenic control mechanism that is not included in the model or by the inherent limitations and sensitivity of the small-scale batch experiments when replicating these complex geochemical reactions. The potential sensitivity to outside influence on the batch experiments has already been identified and proven through the modeling of headspace impacts on the results of the batch experiments pH change tests. Because of this uncertainty, it is accepted that the modeled results will not match the experimental results exactly. The model was able to replicate the observed trend in arsenic removal capacity that was shown in the laboratory experiments and the results suggest that the iron-oxide mechanism of arsenic release and capture. Based on the modeled results as well as the lithology of the site, it is believed to be the primary geochemical mechanism behind the observed arsenic conditions at the Reno-Stead site.

iii. Aquifer Condition Simulation

Modeling of the simplified aquifer conditions provided additional support that iron-oxides are adsorbing and desorbing arsenic in response to changes in pH. Although the dominant water in this model is that of the simulated injection water with a low arsenic concentration, final arsenic concentrations are elevated at all test initial pH values except for pH of 7.5. These results indicate that arsenic is being released from iron-oxide surfaces sites as pH values shift from neutral to more acidic or basic. This mirrors the

results from the iron-oxide reduction model where intermediate pH values showed the highest arsenic sorption capacity. Although injected water with a low arsenic concentration is making up 80% of the total solution present in the model, the dilution of the background 0.037 mg/L arsenic concentration with this low arsenic water is offset and even reversed by the desorption of arsenic from the iron-oxide surfaces present in the aquifer. Only at injected water with pH values ranging from 6.7 to 7.2 is the arsenic concentration able to be reduced and only by 5%. This limited range for injection water pH values is important as any water that is injected at a pH outside this range not only will result in no arsenic dilution, it may contribute to greater arsenic mobilization. During the injection test, injected water had a pH range of 7.09-7.32. Under these field injection pH values, the model predicts a similar final arsenic concentration to that observed at the Reno-Stead site. This match between the model results and the field observations validates the hypothesis that sorption and desorption from iron-oxides in the aquifer is the primary mechanism behind the observed arsenic concentrations at the site.

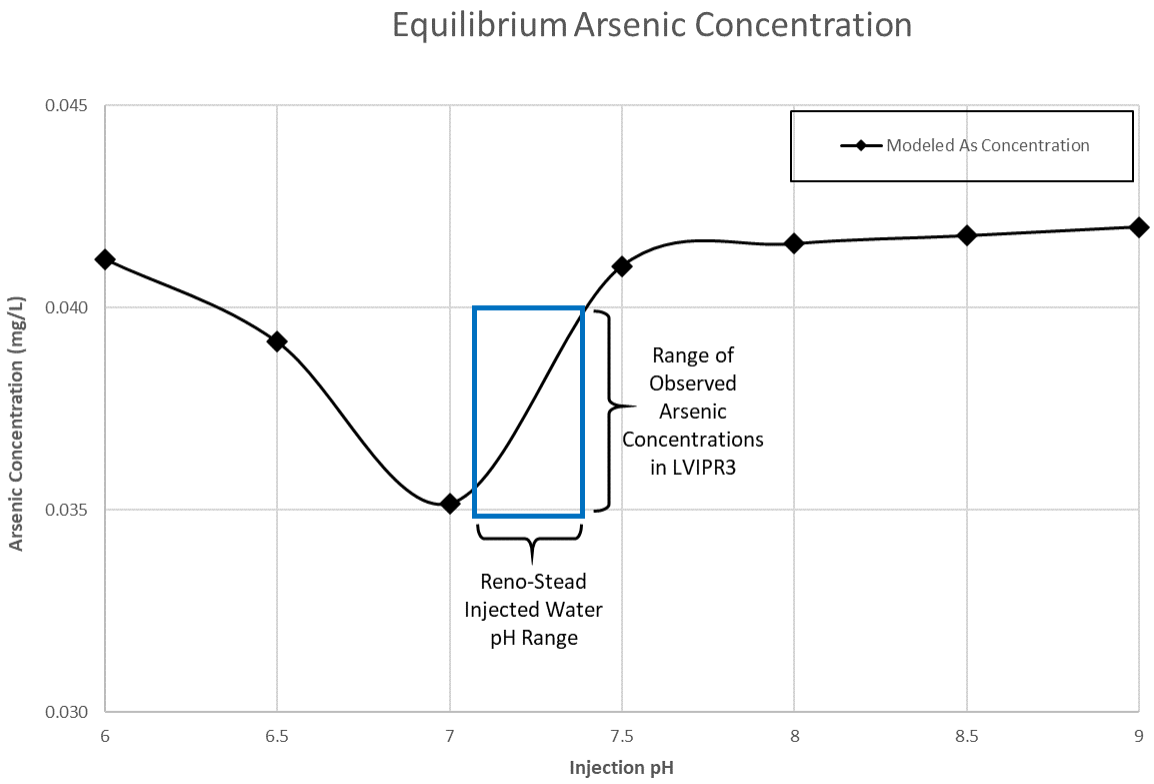

Figure 11.1: Modeled final arsenic concentrations in mg/L after mixing and equilibration of injected water of different pH values and native groundwater. The range of actual injected pH values and observed arsenic concentrations during the injection test at the Reno-Stead site are indicated by the box.

In addition to the impact of injected water pH on arsenic concentrations observed in this model, lead concentrations also showed pH dependence and possible iron-oxide sorption. Concentrations of lead were measured at 1.12 mg/L in the background groundwater at the site and at 0 mg/L in the injected water. Final equilibrium results (Figure 11.2:) showed that at all injected water pH values, lead concentrations decreased. However, at pH values above 7.2, lead concentrations are above the expected dilution ratio. This indicates that although dilution is occurring, some lead release from iron-oxide surfaces is also occurring. pH values in the range from 7.2 to 8.5 result in lead

concentrations below the expected dilution concentration. This indicates that lead sorption is occurring. Above a pH of 8.5 limited sorption or desorption is observed and lead concentrations match the expected dilution concentration. There are few field measurements for lead at the Reno-Stead site after the initial background samples so there are limited field comparisons to be made. The sorption and desorption of lead to iron-oxides has been identified in multiple studies (Benjamin & Leckie, 1981, Sipos *et al.*, 2008) and may be a possible competitor with arsenic for sorption sites (Kanel *et al.*, 2005, Neupane *et al.*, 2014).

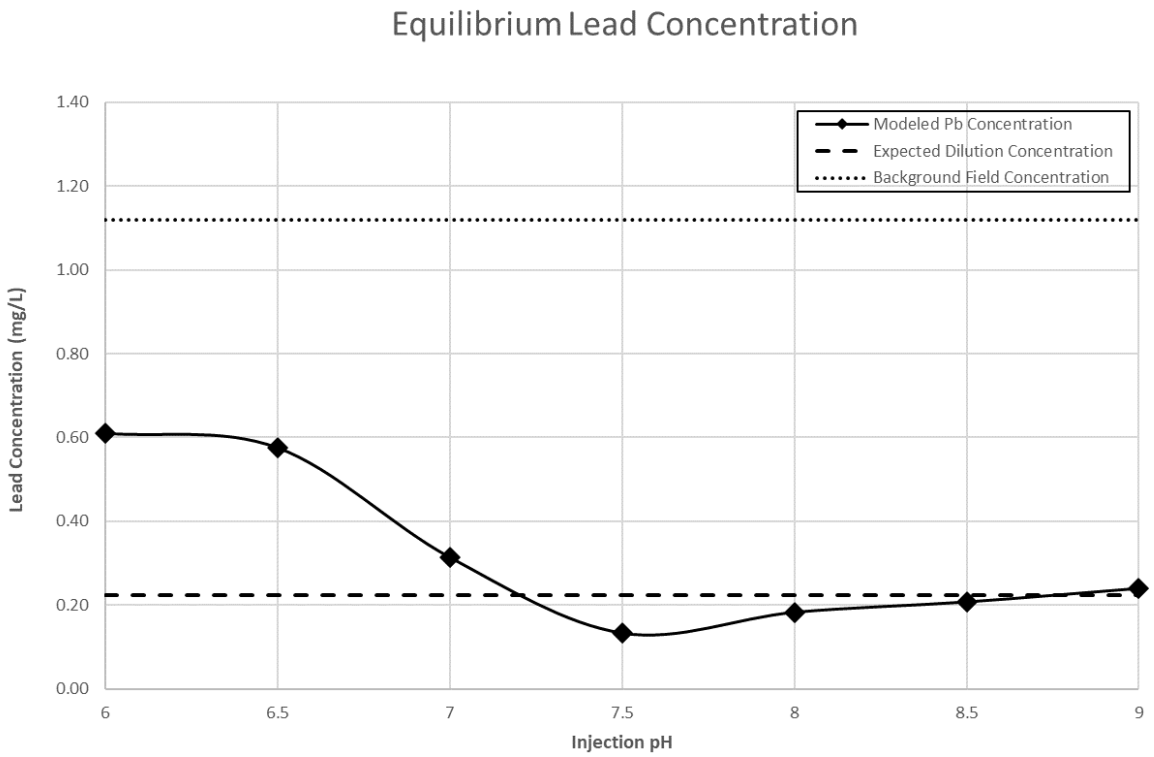

Figure 11.2: Modeled final lead concentrations in mg/L after mixing and equilibration of injected water of different pH values and native groundwater.

To test the hypothesis that iron-oxides are driving the arsenic dynamics observed at the site, the same model was run without the addition of any surface sites available for arsenic sorption or desorption. Under these conditions, arsenic concentration is not impacted by the pH of the injection water. Under all tested injected water pHs, the final arsenic concentrations are at the expected dilution concentrations for 80% injected water and 20% native groundwater of 0.026 mg/L (Figure 11.3). This lack of response to pH changes with the removal of the iron-oxide surfaces on the final arsenic concentrations further supports that iron-oxides are the primary driver for arsenic concentrations at this site.

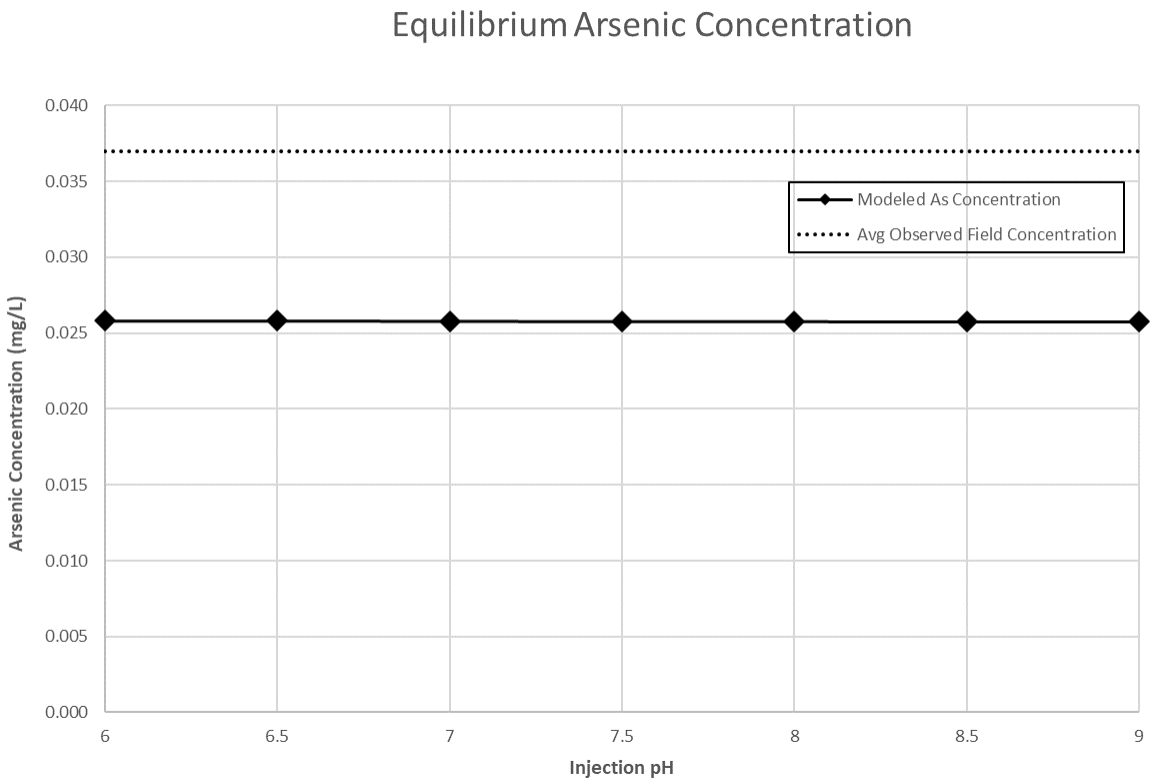

Figure 11.3: Modeled final arsenic concentrations in mg/L after mixing and equilibration of injected water of different pH values and native groundwater without the presence of iron-oxide surfaces.

iv. Limitations

Although the modeled and experimental results support each other, there is still some variation and uncertainty present in this study. One of the primary limitations in generation of this model is the relative simplicity and large number of assumptions that are made when determining model inputs. Because the model was created and validated utilizing the same setup and inputs as the batch experiments, it limits the final model's ability to fully replicate the field conditions observed at the Reno-Stead site. The batch experiments and in turn the model, have a limited scale and cannot accurately take into account the massive heterogeneity that is present under actual aquifer conditions (Sharif

et al., 2008). The batch experiments on which the model is developed were performed at scale that while able to show some of the geochemical reactions are taking place between the aquifer mineralogy and different waters, may also hide some of the secondary reactions that occur due to the scale at which they are performed. The model is a simplified and homogenized interpretation of a real-world system as well. The model does not include all of the potential surface sites that may be having secondary impacts on arsenic controls. The simulated injected and native waters are simplified and normalized for the model and do not match the full water chemistry of the real injected and native groundwater at the site. This may impact the actual efficiency of arsenic sorption at the surface sites as concentrations of other dissolved constituents can compete with arsenic for sorption locations (Stollenwerk *et al.,* 2007). Despite these limitations, the model is able to capture the primary geochemical mechanisms that are occurring at the Reno-Stead site and its results help direct further investigation and identify new questions that can be explored more thoroughly.

Overall Conclusions

a. Arsenic Controls at the Reno-Stead Site

The modeled results from the iron-oxide hypothesis support the hypothesis that the likely source for arsenic at the site is sorbed arsenic to iron-oxides present in the aquifer mineralogy. Arsenic removal capacity observed in this model tracks with the arsenic removal capacity observed during the batch experiments. Additionally, the pH changes observed during the batch experiments help explain how introduction of injection water alters pH in a way that may result in the potential release of arsenic.

Confirming that iron-oxide sorption is the likely source for free arsenic in this system helps explain the initial arsenic concentration variation and then eventual stability that was observed in the extraction well during the injection testing. Because the sorptive capacity of iron-oxides is impacted by pH, as pH increased during injection, the sorptive capacity was reduced and arsenic was released into the groundwater. As the sorptive capacity was reduced by the change in pH from injection, the dilution that was occurring following the introduction of low arsenic injected water was offset by the release of previously sorbed arsenic. This conclusion is supported by the results of the aquifer simulation model. At initial pH values the are between 6.5 and 7.5, arsenic sorption remains relatively stable, but enough desorption occurs to offset any dilution that is occurring from the introduction of low arsenic injected water. This iron-oxide sorption/desorption interaction with arsenic at these intermediate pH values help explain the near constant elevated arsenic concentrations that were observed during the injection test at the Reno-Stead site.

Additionally, the discovery of pH impact on lead concentrations may also impact our understanding of arsenic at the site. Although understanding the geochemical mechanisms behind lead concentrations at the site was not the primary goal of the model, the observed pH impact on lead creates a new set of questions that could be explored utilizing this model framework. The potential competition between lead and arsenic at the site may impact the viability of potential mitigation strategies and needs to be evaluated further.

b. Importance and Future Applications

In all groundwater recharge projects and particularly in those utilizing treated, reclaimed water, it is important to ensure that no adverse impacts to native groundwater or injected water chemistry occurs. This is a primary hurdle in determining the viability of future ASR projects in the region. Ultimately, the goal of ASR projects is to support existing groundwater supplies or potentially increase them. If water quality is degraded during this process, the resource is unusable. By proving that this geochemical model approach is both accurate and useful, it creates another tool as well as another safeguard when assessing future ASR sites.

While this model framework does not entirely replace or eliminate the need for field observations or batch experiments in determining compatibility of these waters, it can help identify potential issues that may need more rigorous investigation. By developing this type of geochemical model upfront any potential risks can be identified, and new areas of inquiry opened. This allows for directed and purposeful exploration of some of the issues that the model identified before full-scale sign on to projects occur.

Additionally, this model framework allows for the potential of testing various mitigation methods such as changing injected water pH or adding minerals to the injected water before injection to reduce the potential for undesirable interactions with the native geology. The ability of the model to test all of these scenarios before any water is injected greatly improves the likelihood that future ASR projects are successful.

c. Future Work and Further Development

While the simple geochemical model developed in this study looked to answer the question of arsenic source at this site, it limited the potential of the model to help identify

other potential issues. Arsenic was a known contaminant at the Reno-Stead site and the development of this model was able to utilize a large number of field data points for validation and was tailored specifically to arsenic. This geochemical model framework can and should be developed further to provide insight into not only a single potential harmful constituent but into multiple, potentially unknown constituents. In many potential future applications, there may be few to no field measurements available. There may be multiple constituents of concern instead of just one. In order to properly address the challenges faced in more complex situations, the geochemical model framework that has been outlined needs to be developed further. For this development to occur, additional sites must be identified and modeled. These sites might have limited amounts of field data available and may have multiple risks of potential geochemical incompatibility present. By further testing and tweaking of this basic framework, the minimum levels of inputs for the model to be useful can be identified and fewer and fewer resources will be needed to create a reliable and useful model. From this model, the next line of questioning can be developed and specific, directed investigation can occur. This is the ultimate goal as it allows for the most cost-effective, streamline and accurate method of testing and implementing future ASR projects.

References

Ahmad, A. & Bhattacharya, P. (2019) Arsenic in Drinking Water: Is 10 µg/L a Safe Limit? *Curr. Pollut. Rep.* 5(1), 1–3. Springer. doi:10.1007/s40726-019-0102-7

Appelo, C. A. J. & Vet, W. W. J. M. de. (2003) Modeling in situ iron removal from groundwater with trace elements such as. In: *Arsenic in Ground Water* (A. H. Welch & K. G. Stollenwerk, eds.), 381–401. Boston, MA: Springer US. doi:10.1007/0-306-47956-7_14

Ball, J. W. & Nordstrom, D. K. (1991) User's manual for WATEQ4F, with revised thermodynamic data base and text cases for calculating speciation of major, trace, and redox elements in natural waters (Report No. 91–183). Open-File Report, Version 2.0. doi:10.3133/ofr91183

Benjamin, M. M. & Leckie, J. O. (1981) Multiple-site adsorption of Cd, Cu, Zn, and Pb on amorphous iron oxyhydroxide. *J. Colloid Interface Sci.* 79(1), 209–221. doi:10.1016/0021-9797(81)90063-1

Cordy, G. E. & Szecsody, James. (1985) Reno NE quadrangle : earthquake hazards map. Earthquake hazards map of the Reno NE quadrangle. Reno, Nev: Nevada Bureau of Mines and Geology, University of Nevada-Reno.

Currell, M., Cartwright, I., Raveggi, M. & Han, D. (2011) Controls on elevated fluoride and arsenic concentrations in groundwater from the Yuncheng Basin, China. *Appl. Geochem.* 26(4), 540–552. doi:10.1016/j.apgeochem.2011.01.012

Dillon, P., Pavelic, P., Toze, S., Rinck-Pfeiffer, S., Martin, R., Knapton, A. & Pidsley, D. (2006) Role of aquifer storage in water reuse. *Desalination* 188(1–3), 123–134. doi:10.1016/j.desal.2005.04.109

Drewes, J. E., Reinhard, M. & Fox, P. (2003) Comparing microfiltration-reverse osmosis and soil-aquifer treatment for indirect potable reuse of water. *Water Res.* 37, 3612–3621. doi:10.1016/S0043-1354(03)00230-6

Dzombak, D. A. & Morel, F. (1990) *Surface complexation modeling : hydrous ferric oxide*. New York: Wiley.

Fakhreddine, S., Dittmar, J., Phipps, D., Dadakis, J. & Fendorf, S. (2015) Geochemical Triggers of Arsenic Mobilization during Managed Aquifer Recharge. *Environ. Sci. Technol.* 49(13), 7802–7809. doi:10.1021/acs.est.5b01140

Ferguson, J. F. & Gavis, J. (1972) A review of the arsenic cycle in natural waters. *Water Res.* 6(11), 1259–1274. doi:10.1016/0043-1354(72)90052-8

Gotkowitz, M. B., Schreiber, M. E. & Simo, J. A. (2004) Effects of water use on arsenic

release to well water in a confined aquifer. *Ground Water* 42(4), 568–575. doi:10.1111/j.1745-6584.2004.tb02625.x

Hafeznezami, S., Lam, J. R., Xiang, Y., Reynolds, M. D., Davis, J. A., Lin, T. & Jay, J. A. (2016) Arsenic mobilization in an oxidizing alkaline groundwater: Experimental studies, comparison and optimization of geochemical modeling parameters. *Appl. Geochem.* 72, 97–112. doi:10.1016/j.apgeochem.2016.07.011

Harrill, J. R. (n.d.) Evaluation of the water resources of Lemmon Valley, Washoe County, Nevada, with emphasis on effects of ground-water development to 1971, by James R. Harrill. 1.

Hinkle, S. R. & Polette, D. J. (1999) Arsenic in Ground Water of the Willamette Basin, Oregon. *US Geol. Surv.*

Jang, Y.-C., Somanna, Y. & Kim, H. (2016) Source, Distribution, Toxicity and Remediation of Arsenic in the Environment – A review. *Int. J. Appl. Environ. Sci. ISSN* 11(2), 973–6077.

Jones, G. W. & Pichler, T. (2007) Relationship between pyrite stability and arsenic mobility during aquifer storage and recovery in southwest central Florida. *Environ. Sci. Technol.* 41(3), 723–730. doi:10.1021/es061901w

Kanel, S. R., Manning, B., Charlet, L. & Choi, H. (2005) Removal of Arsenic(III) from Groundwater by Nanoscale Zero-Valent Iron. *Environ. Sci. Technol.* 39(5), 1291–1298. doi:10.1021/es048991u

Masue, Y., Loeppert, R. H. & Kramer, T. A. (2007) Arsenate and Arsenite Adsorption and Desorption Behavior on Coprecipitated Aluminum:Iron Hydroxides. *Environ. Sci. Technol.* 41(3), 837–842. doi:10.1021/es061160z

Mosier, E. L., Papp, C. S. E., Motooka, J. M., Kennedy, K. R. & Riddle, G. O. (1991) Sequential Extraction Analyses of Drill Core Samples, Central Oklahoma Aquifer (Open-File Report). Open-File Report.

Neupane, G., Donahoe, R. J. & Arai, Y. (2014) Kinetics of competitive adsorption/desorption of arsenate and phosphate at the ferrihydrite–water interface. *Chem. Geol.* 368, 31–38. doi:10.1016/j.chemgeo.2013.12.020

Nickson, R. T., Mcarthur, J. M., Ravenscroft, P., Burgess, W. G. & Ahmed, K. M. (2000) Mechanism of arsenic release to groundwater, Bangladesh and West Bengal. *Appl. Geochem.* 15(4), 403–413. doi:10.1016/S0883-2927(99)00086-4

Parkhurst, D. L. & Appelo, C. A. J. (2013) Description of input and examples for PHREEQC version 3: a computer program for speciation, batch-reaction, one-dimensional transport, and inverse geochemical calculations (Report No. 6-A43). Techniques and Methods, 519. Reston, VA. doi:10.3133/tm6A43

Perez, L. J. (2020) Modeling geochemical evolution of groundwater at the Reno-Stead site.

Podgorski, J. E., Eqani, S. A. M. A. S., Khanam, T., Ullah, R., Shen, H. & Berg, M. (2017) Extensive arsenic contamination in high-pH unconfined aquifers in the Indus Valley. *Sci. Adv.* 3(8), 1–10. doi:10.1126/sciadv.1700935

Pohll, G., White, N. & Pullammanappallil, S. (2019) RSWRF Characterization Report Nov_22_2019.

Raven, K. P., Jain, A. & Loeppert, R. H. (1998) Arsenite and Arsenate Adsorption on Ferrihydrite: Kinetics, Equilibrium, and Adsorption Envelopes. *Environ. Sci. Technol.* 32(3), 344–349. doi:10.1021/es970421p

Robinson, C., Brömssen, M. von, Bhattacharya, P., Häller, S., Bivén, A., Hossain, M., Jacks, G., et al. (2011) Dynamics of arsenic adsorption in the targeted arsenic-safe aquifers in Matlab, south-eastern Bangladesh: Insight from experimental studies. *Appl. Geochem.* 26(4), 624–635. doi:10.1016/j.apgeochem.2011.01.019

Sharif, M. U., Davis, R. K., Steele, K. F., Kim, B., Kresse, T. M. & Fazio, J. A. (2008) Inverse geochemical modeling of groundwater evolution with emphasis on arsenic in the Mississippi River Valley alluvial aquifer, Arkansas (USA). *J. Hydrol.* 350(1–2), 41–55. doi:10.1016/j.jhydrol.2007.11.027

Sipos, P., Németh, T., Kis, V. K. & Mohai, I. (2008) Sorption of copper, zinc and lead on soil mineral phases. *Chemosphere* 73(4), 461–469. doi:10.1016/j.chemosphere.2008.06.046

Smedley, P. L. & Kinniburgh, D. G. (2002) A review of the source, behaviour and distribution of arsenic in natural waters. *Appl. Geochem.* 17(5), 517–568. doi:10.1016/S0883-2927(02)00018-5

Stollenwerk, K. G., Breit, G. N., Welch, A. H., Yount, J. C., Whitney, J. W., Foster, A. L., Uddin, M. N., et al. (2007) Arsenic attenuation by oxidized aquifer sediments in Bangladesh. *Sci. Total Environ.* 379(2–3), 133–150. doi:10.1016/j.scitotenv.2006.11.029

Vaughan, D. J. (2006) Arsenic. *Elements* 2(2), 71–75. GeoScienceWorld. doi:10.2113/gselements.2.2.71

Wallis, I., Prommer, H., Pichler, T., Post, V., B. Norton, S., Annable, M. D. & Simmons, C. T. (2011) Process-based reactive transport model to quantify arsenic mobility during aquifer storage and recovery of potable water. *Environ. Sci. Technol.* 45(16), 6924–6931. doi:10.1021/es201286c

Wallis, I., Prommer, H., Simmons, C. T., Post, V. & Stuyfzand, P. J. (2010) Evaluation of conceptual and numerical models for arsenic mobilization and attenuation during

managed aquifer recharge. *Environ. Sci. Technol.* 44(13), 5035–5041. doi:10.1021/es100463q

Welch, A. H. & Lico, M. S. (1998) Factors controlling As and U in shallow ground water, southern Carson Desert, Nevada. *Appl. Geochem.* 13(4), 521–539. doi:10.1016/S0883-2927(97)00083-8

White, N. & Pohll, G. (2020) Arsenic Concentration Variability at the Reno-Stead Demonstration Site.

Yao, S., Liu, Z. & Shi, Z. (2014) Arsenic removal from aqueous solutions by adsorption onto iron oxide/activated carbon magnetic composite. *J. Environ. Health Sci. Eng.* 12(1), 6–13. doi:10.1186/2052-336X-12-58

Zhu, N. (2012) *Geochemical Modeling of an Aquifer Storage and Recovery Project in Union County , Arkansas*.